IDENTIFYING PEPTIDE SENSORS FOR HIGHLY CURVED MEMBRANES AND LIPID COMPONENTS

by

LESLIE ANNE MORTON

B.S, University of North Carolina, 2008

A thesis submitted to the Faculty of the Graduate School of the University of Colorado in partial fulfillment of the requirement for the degree of

Doctor of Philosophy

Department of Chemistry and Biochemistry

2013

This thesis entitled:

IDENTIFYING PEPTIDE SENSORS FOR HIGHLY CURVED MEMBRANES AND LIPID COMPONENTS

Written by Leslie Anne Morton

has been approved for the Department of Chemistry and Biochemistry

_____

PhD Thesis Adviser Hang Yin, Ph.D.

_____

Professor Natalie G. Ahn, Ph.D.

Date:_____

The final copy of this thesis has been examined by the signatories, and we find that both the content and the form meet acceptable presentation standards of scholarly work in the above mentioned discipline.

Morton, Leslie A. (Ph.D., Biochemistry)

IDENTIFYING PEPTIDE SENSORS FOR HIGHLY CURVED MEMBRANES AND LIPID COMPONENTS

Thesis directed by Associate Professor Hang (Hubert) Yin, Ph.D.

Membrane curvature is a vital function in several significant biological processes. Indeed, this behavior is critical for activating certain signaling processes, membrane budding for endocytosis and exocytosis, membrane fusion and transporting molecules across the membrane. Membrane curvature triggers the activation of specific proteins that specifically target positively curved membranes, i.e. Caveolin-1, Amphiphysin, Synaptotagmin-1, ARF GTPase activating protein (ARFGAP1), and other proteins containing Bin/Amphiphysin/Rvs (BAR) domains. These proteins carry out important behaviors for proper cellular function. There is currently a need to further investigate the biophysical interactions involved between these proteins and highly curved membranes to further understand their biological behaviors. Furthermore, lipid composition has also been reported to influence membrane curvature targeting as its shape and charge gives it a specific behavior within the bilayer. Lipids have an important role of maintaining the cellular mobility and shape, where certain lipids can generate bilayer accessibility, initiating bilayer insertion of specific moieties of proteins and peptides.

Highly curved membranes are not only found as undulations and indentions on the surface of cells and cellular organelles but also can be identified as nano-sized extracellular vesicles (EVs) that shed from cells. These shed EVs are commonly recognized as microvesicles (d = 100-1000 nm) and exosomes (d = 30-100 nm). Their primary function involves traveling to distal parts of the body for cellular communication via protein-protein or membrane-membrane interaction, carrying proteins and nucleic acids from the cells they were derived from. Most interestingly, these EVs are highly expressed in bodily fluids of patients with metastatic cancer. Currently, there is a need to develop a noninvasive tool to effectively and specifically target these EVs. With an understanding of membrane curvature, we identified a peptide derived from the effector domain (ED) of the membrane protein Myristoylated Alanine-Rich C-Kinase Substrate, formally known as MARCKS-ED, which was observed to target highly curved membranes similar to known protein curvature sensors. Following this observation, we focused on applying this peptide to targeting biological EVs as a potential probe to study cancer progression as well as gaining more knowledge on the biophysical interactions involved with membrane curvature sensing.

In chapter 1, membrane curvature is introduced and its significance is thoroughly discussed. Specific proteins known to target membrane curvature are also described as well as our interest in further understanding these protein-membrane interactions. Our approach to use the MARCKS-ED peptide is explained as well as our project goal to use its potential in

translating its curvature sensing behavior to a biotechnology application. In chapter 2, a detailed protocol on how to effectively prepare and extrude synthetic lipid vesicles is described. This technique is performed prior to any *in vitro* binding assay and is critical in preparing homogenous vesicle solutions. Producing distinct vesicle sizes using a pressured extruder gives validity and confidence to our curvature sensing studies. This established protocol is thus significant to this work. Chapter 3 discusses our novel findings of identifying curvature sensing behavior by the MARCKS-ED peptide using *in vitro*, *in vivo* and *ex vivo* experiments. Fluorescence assays display MARCKS-ED's distinct curvature sensing behavior comparable to known curvature sensing proteins using synthetic lipid vesicles. Using a robust technique to track and analyze nanoparticles in real time further revealed MARCK-ED's ability to bind to stress-induced rat secreted positively curved vesicles, e.g. EVs. These findings led us to further investigate how MARCKS-ED interacts and prefers highly curved vesicles to flatter ones since this behavior was not fully understood. In chapter 4, our approach focuses on biophysically characterizing the specific factors such as Phe residue insertion and lipid composition that contribute to curvature sensing behavior in hopes of further understanding this preferential targeting observed by MARCKS-ED. These results were based on biophysical evidence supporting a molecular dynamics simulation model of how MARCKS-ED may be inserting into the membrane of highly curved synthetic vesicles. Chapter 5 discusses the current conclusions of this work as well as the future works that will be explored as it describes the potential directions

of this project to further understand membrane curvature in hopes of significantly contributing to this field.

Acknowledgements:

I would first like to acknowledge my Ph.D. thesis adviser Hang (Hubert) Yin. With his guidance and leadership, I have been able to successfully complete my doctorate degree. Furthermore, I would like to honorably mention my fellow committee members: Drs. Natalie Ahn, Amy Palmer, Joseph Falke and Ding Xue. They have given me ample amount of ideas and suggestions to help support my research and I am truly grateful for their great knowledge, expertise and assistance. I also would like to thank both Drs. Deborah Wuttke and Robert Batey for their mentorship and believing in me through my struggles at the beginning of my Ph.D. career. Without their encouragement and help, I would not have been able to complete this degree.

There are former members from the Yin lab that require special thanks from me as well. They are Drs. Jonel Saludes, Deanne Sammond and Catherine Joyce. These postdoctoral fellows were instrumental in guiding my research as well as teaching me how to become a better scientist. I appreciate what they have done for me and am thankful for each of their contributions to my research. I must also mention Dr. Annette Erbse who taught me how to use a new instrument in order to optimize a method, record data, and analyze the results throughout the course of a year. I am truly indebted to her for her wisdom and patience.

I would also like to personally thank members of my family. First, my parents, John and Glenys Morton, for supporting my decision to move so far away from home. They have always

believed in me and look forward to the things I will accomplish in the future. I have to give a special acknowledgement to my brother Jason Morton who is the complete opposite of me in both personality and professional interest but has always conveniently given me great pep talks to overcome frustrating times in my research. My family has always been part of the foundation for my motivation to successfully complete my Ph.D. degree, and I feel honored to dedicate this success to them.

Table of Contents

List of Tables

List of Figures

List of Schemes

List of Equations

CHAPTER 1

Membrane Curvature, Nano-sized Extracellular Vesicles and the MARCKS-ED Peptide.

INTRODUCTION

1.1 Membrane Curvature.

The cellular membrane behaves in specific ways that require mobility for functionality. This behavior includes surface undulations that produce membrane protrusions of positive and negative curvature. Significantly, this action is important in conducting cellular functions, which include triggering endocytosis and exocytosis, regulating the transport of molecules across the membrane bilayer, and stimulating membrane fusion and cellular division (*1*). Membrane curvature, defined as the reciprocal of the cellular diameter, is regulated through specific proteins to carry out these necessary cellular functions. Lipid domains have also been reported to be an influence on membrane curvature and play an integral role in recruiting these specific protein motifs and domains for membrane interaction (*1*). The curvature of membranes is the consequence of both lipid domains and protein domains synergistically altering the membrane topology and shape (*2*). In fact, detailed studies have reported specific categories that modify membrane deformation: (1) changes in lipid composition, (2) integral proteins that have intrinsic curvature or curvature based on oligomerization, (3) changes in cytoskeleton polymerization, (4)

direct and indirect scaffolding of the membrane bilayer and (5) amphipathic helix insertion into the outer membrane leaflet. Due to the inability to measure membrane curvature *in vivo*, current studies on membrane curvature are primarily *in vitro* (*2*). Our studies stem from a current need to understand further factors involved with protein interactions with highly curved membrane surfaces.

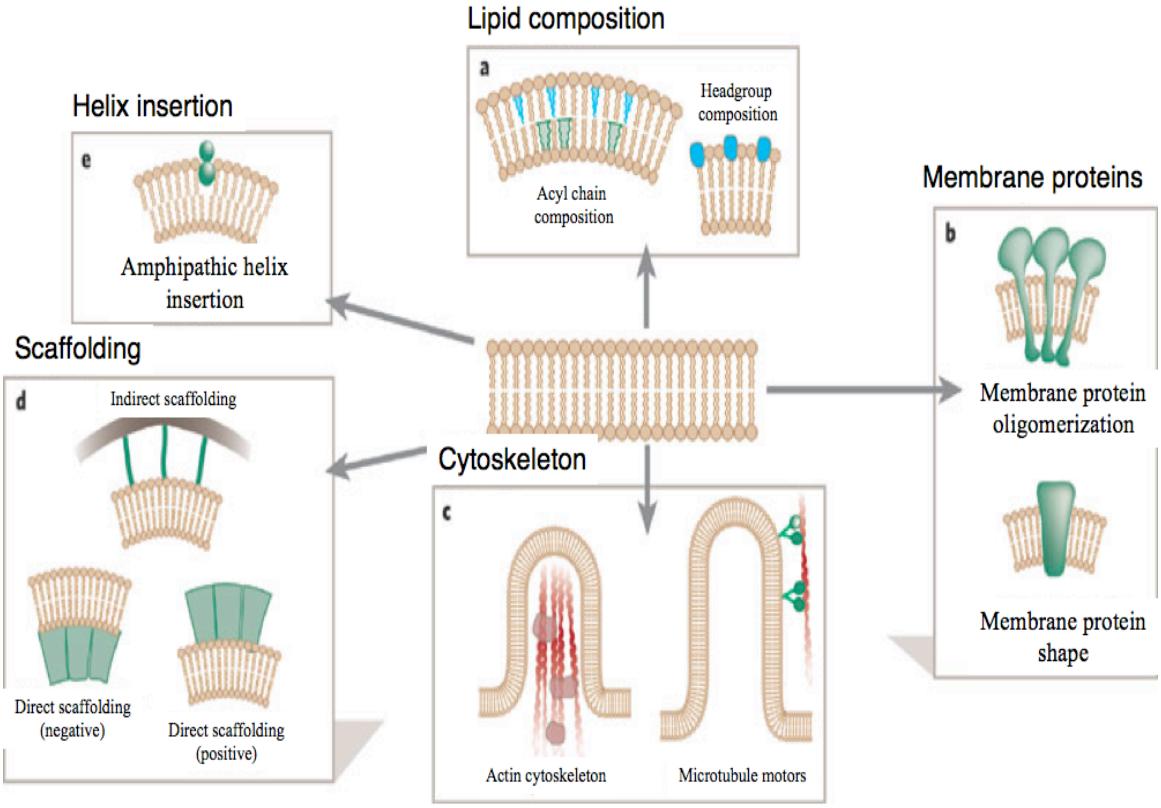

Scheme 1.1 Schematic showing different attributes of membrane curvature. Membrane curvature is observed on the surface of the cell as undulations or wave-like bends that form positive and negatively curved regions. This detailed depiction of membrane curvature is courtesy of Gallop et al (*1*).

1.2 Commonalities of Membrane Curvature Sensing Proteins.

Membrane curvature sensing proteins have distinct functions within the cell ranging from fusing membranes to triggering neuronal exocytosis (*3*). Many of these curvature sensing proteins exhibit the behavior of inducing membrane curvature, the "active" behavior of modulating the membrane shape through energy. Specifically, many of these proteins contain the Bin/Amphiphysin/Rvs (BAR) domain with an amphipathic helix preceding the BAR domain on the N-terminus, which is induced upon membrane binding (*3*). However, reports have identified commonalities among these curvature sensing proteins for sensing membrane curvature: a "passive" behavior of membrane curvature interaction. These requirements are reported as including insertion moieties, such as (1) hydrophobic residues or amphipathic helices, and (2) surface membrane stabilization, proposing the significance of electrostatic interactions and membrane scaffolding (*2*). Although it is reported that lipids also have an influence on curvature sensing behavior, the BAR domain is one of the most studied protein motifs to study these specific proteins involved with curvature sensing.

More specifically, Synaptotagmin-1, a protein responsible for membrane fusion for synaptic release in the presence of Ca^{2+} is known to 'sense' curvature, its passive behavior, via membrane insertion by its two tandem C2 domains- C2A and C2B (*3*). The accessory human immunodeficiency virus-1 (HIV) Nef protein, responsible for viral replication and the

advancement to acquired immunodeficiency syndrome (AIDS), interacts with the membrane based on membrane curvature, lipid composition, surface electrostatic interactions and hydrophobic insertion (*4*). Furthermore, a lipid-packing sensor (ALPS) in ARF GTPase-activating protein 1 (ARFGAP1), responsible for protein coat assembly (*2*), has been linked to interacting to highly curved membranes based on lipid motifs sensitive to defects in lipid packing (*5*). BAR domain-containing proteins, such as Amphiphysin and Endophilin-A1, have been characterized to sense membrane curvature based on the interaction between the negatively-charged membrane and the positively-charged concave-oriented domain of the protein via protein scaffolding (*6*), hydrophobic insertion and lipid packing defects exposed on the membrane surface (*7*). In summary, with the exception of lipid composition influence, these proteins exhibit similar intrinsic properties required for curvature sensing behavior, including (a) hydrophobic residue insertion and (b) membrane surface stabilization, in the form of either electrostatic interactions or protein scaffolding.

1.3 The Discovery of Extracellular Vesicles and their Highly Curved Membranes.

Extracellular vesicles (EVs) are membrane-enclosed sacs that shed from both normal and cancer cells. They are identified as nano-sized vesicles ranging from 30 - 100 nm in diameter, described as exosomes and 100 nm - 1 μM in diameter described as microvesicles. These EVs have attracted even more interest as it was discovered that an overexpression of microvesicles was observed in those with metastatic cancer, specifically describing the propensity of cancer to spread. It has also been reported that the amount of microvesicles released from cancer cells has

been correlated to its invasive behavior both *in vitro* and *in vivo* (*8*). Indeed a few decades ago, microvesicles were first documented in 1978 in cancer patients with Hodgkins disease (*9*). Following this discovery, microvesicles were observed to spontaneously shed from highly metastatic B16 mouse melanoma cells. These shed microvesicles were then fused to weakly metastatic B16 mouse melanoma cells where it was documented that the weakly metastatic B16 cells began to metastasize to the lung (*9, 10*). These early studies laid the foundation of further investigations to focus on the correlation between microvesicle shedding and cancer progression.

1.4 The Roles of Extracellular Vesicles.

Recently, it has been accepted that extracellular vesicle shedding is no longer considered an artefact (*11*). These vesicles indeed have a function and carry out important biological roles. These membrane-enclosed vesicles consist of a lipid composition distinct from the cellular plasma membrane it was shed from (*9*). EVs are identified by two subgroups based on (a) vesicle diameter size and (b) mode of excretion from the derived cell (*9*). Exosomes are secreted into the extracellular matrix from multivesicular bodies (MVBs) following invagination by the cell. By contrast, microvesicles undergo a budding mechanism from the plasma membrane similar to the abscission step in cytokinesis (*9*). The budding behavior of the plasma membrane is known to be induced by proteins altering the membrane curvature or lipid asymmetry. In fact, lipid de-regulation is proposed to be an initiator of the over-exposure of phosphatidylserine (PS) present on the outer leaflet of the plasma membrane. These EVs include several functions; as the most

studied function is cell-to-cell communication. EVs, both microvesicles and exosomes, that shed from tumor cells, travel through bodily fluids, such as urine, blood and ascitic tissue carrying cargo specific to the cell from which it was derived from. EVs have been observed to carry out the following functions: (1) promoting angiogenesis by carrying VEGF and miRNAs that modulate endothelial cells, (2) evading the immune system by fusing with other immune cells or by the over-exposure of phosphatidylserine (PS) on its outer leaflet, (3) invading target cells by utilizing proteases it may be carrying to degrade the matrix surrounding other cells, (4) transferring oncogenic receptors to other cells, (5) resisting potential drugs by utilizing the membrane-vesicle as a way to efflux potential chemotherapy drugs from the cell and (6) modulating the environment to promote tumor growth and survival (*9*).

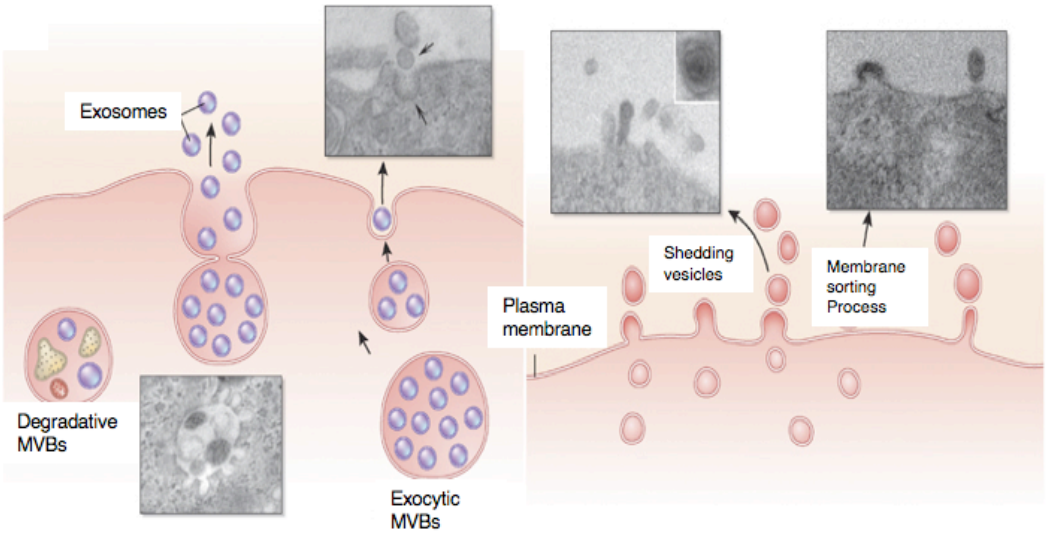

Scheme 1.2 Schematic describing the secretion mechanism of exosomes and microvesicles. Nano-sized extracellular vesicles, collectively recognized as exosomes and microvesicles, shed from cells into the extracellular matrix and travel through bodily fluids to target other cells. Their interaction with targeted cells range from protein-protein interaction and membrane-membrane

interaction. This figure is a clear depiction of extracellular excretion courtesy of Biancone et al (*12*).

1.5 Extracellular Vesicles as Biomarkers of Cancer Progression.

This section is a reformatted excerpt of the following paper:

Morton, L. A.; Coulup, S. K.; Saludes, J. P. and Yin, H. (2012) Biomarkers beyond proteomics and genomics: microvesicles as indicators of cancer progression. BioTech International (BTI). (SeptOct issue).

Protein and gene-based biomarkers are critical indicators for evaluating certain biological processes that give insight into the patient's pathologic condition; however, only a few of these candidate biomarkers have progressed beyond the initial stage and many are plagued with problems including failed translation to bedside care and poor specificity which lead to many false-positive results. The discovery that microvesicles shed by cancer cells are released in bodily fluids has paved the way to a paradigm shift in biomarker detection. The ability to target and study these nanovesicles using designed synthetic peptides is valuable in helping clinicians and patients with treatment decisions and improving the quality of personalized medicine.

The particle size and the exposure of phosphatidylserine on the vesicle membrane surface are the two properties that distinguish microvesicles from normal cells, potentially providing a strategy for specific targeting. No longer considered an artifact, these microvesicles have the

potential to function as a biomarker, paving the way to identify peptide probes for the detection of metastatic behavior- pivotal due to the high incidences of cancer metastasis-related deaths. Since these nano-sized lipid vesicles are ultramicroscopic, there is a need for new technology to detect these potential metastatic cancer biomarkers. Flow cytometry, electron microscopy and dynamic light scattering all have instrument limitations that hinder their capability for accurate vesicle counting on the nanoscale (*13*). Our approach is to design peptides with a conjugated fluorophore to specifically target these vesicles using different techniques, which are performed to identify peptide-bound lipid vesicles. Using small peptides to select for these EVs is due to their feasibility and minimally invasive properties.

With different techniques, we have demonstrated the ability to detect highly curved vesicles using a synthesized natural peptide. Motifs from other curvature sensing proteins have been investigated to improve the selection for nanovesicles. These motifs include insertion moieties and electrostatic stabilization; features presumably necessary for identifying and designing other curvature sensing peptides. Further development of this peptide technology holds great promise for new biomarker detection methods beyond the traditional proteomic and genomic approach.

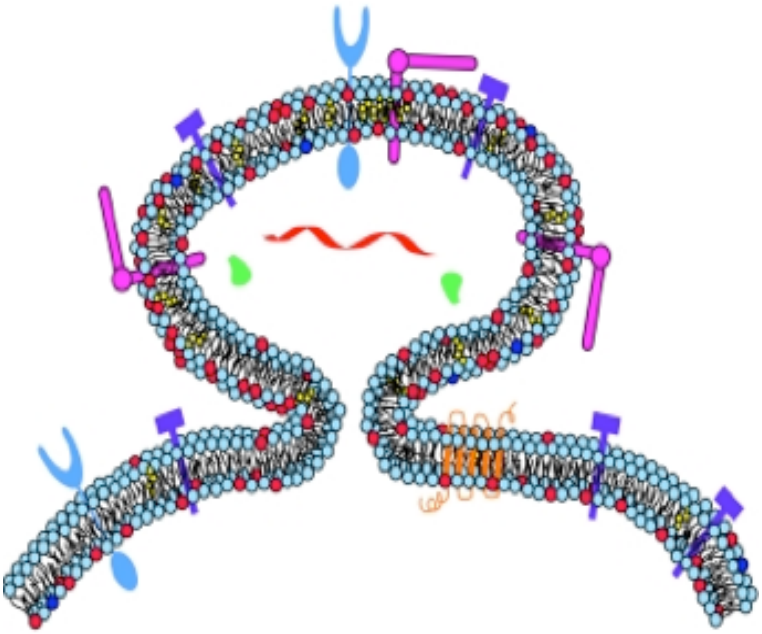

Scheme 1.3 Schematic showing a highly curved microvesicle. Extracellular vesicles are currently being investigated as potential biomarkers to study cancer progression. Our work hopes to use novel ways to detect biologically relevant, highly curved vesicles based on our knowledge on targeting positive membrane curvature and lipid compositions using peptides. Courtesy of D'Souza-Schorey et al. (*9*).

1.6 Introduction to the MARCKS-ED Protein and Peptide.

The Myristoylated Alanine-Rich C-Kinase Substrate (MARCKS) protein is an 87-kDa, natively, unfolded cytoplasmic membrane protein known to interact with multiple targets to activate and inhibit certain signaling pathways. Based on its name, the N-terminus inserts into the membrane following myristoylation, suggesting a way to stabilize interactions between MARCKS and the membrane at the aqueous-lipid head group interface. Beyond the N-terminus, the

phosphorylation site domain (PSD) or the effector domain (ED) has been shown to undergo an insertion mechanism into the membrane (*14*). Its cellular concentration is reported to be 10 μM in neuronal tissue (*14, 15*). The effector domain (ED) is identified as the specific region of the protein known to interact with the inner leaflet of the plasma membrane, commonly recognized as MARCKS-ED. This region is prominently understood to sequester three acidic lipid molecules, phosphatidylinositol 4,5-bisphosphate (PIP_2), on the cytosolic inner leaflet (*15*). This interaction subsequently inhibits phospholipase-C from catalyzing PIP_2 to produce substrates inositol trisphosphate (IP_3) and diacylglycerol (DAG) (*16*).

Furthermore, upon MARCKS-ED's release of the membrane, the effector domain has been observed to bind to Calcium-bound Calmodulin (Ca^{2+}-CaM) at nanomolar affinity. There is currently no crystal structure for the full MARCKS protein or MARCKS-ED peptide; however, there is one displaying a short sequence from the effector domain with Calcium-bound Calmodulin. Through X-ray crystallography, a crystal structure with 2 Å resolution displays a truncated MARCKS-ED region adopting a 'short helical region' when bound to Ca^{2+}-CaM (*17*). It is commonly reported and confirmed by our own biophysical characterization through circular dichroism that the full MARCKS-ED peptide adopts an elongated, unstructured secondary structure in the absence and presence of lipids. For these crystallographic studies, the complete 25-residue MARCK-ED (a.a. 150-175) peptide was not presented in the structure because they were unable to co-crystallize the peptide with the Ca^{2+}-CaM complex. So this structure presents the sole available structure associated with the MARCKS-ED protein as a truncated 19-residue (a.a. 148-166) peptide (*17*).

MARCKS is also a protein kinase C (PKC) substrate where its Ser residues within the effector domain are phosphorylated in the brain and in other tissues (*18*). Phosphorylation decreases electrostatic interactions between MARCKS-ED with the acidic PIP_2 lipids located on the inner leaflet membrane, approximately 1000-fold reportedly (*14*). This action consequently translocates MARCKS-ED to the cytoplasm, which in turn, re-activates Phospholipase-C signaling for PIP_2 catalysis (*19, 20*).

1.7 Introduction to other newly identified curvature sensing peptide probes

Our curvature sensing studies have also identified two other curvature sensing peptide probes known to have dynamic interactions with the membrane. These works were led by Dr. Jonel P. Saludes. One of these peptides was derived from the Synaptotagmin-1 (Syt-1) protein, an integral part of the N-ethylmaleimide-sensitive factor Attachment protein Receptor (SNARE) complex involved with membrane fusion. This peptide, defined as C2B and described as DYDKIGKNDA, was synthesized from loop 3 of the C2B domain; one of two C2 domains of the cytoplasmic protein observed to penetrate into the membrane bilayer upon calcium binding. This peptide was chosen due to its ability to target highly curved membranes upon calcium binding. Surprisingly, no curvature sensing behavior was observed with the linear from of the peptide; however, further studies were performed to modify the peptide's structural conformation. It was shown that decreasing peptide mobility through peptide cyclization to loosely mimic the constraints it would possess within the full protein resulted in curvature sensing behavior.

Despite how peptide rigidity may have had an effect on how the C2B peptide targets highly curved membranes, multivalency may also be a significant component for identifying another curvature sensing peptide probe. A 10 a.a. peptide derived from the membrane protein Bradykinin was synthesized based on observations of its membrane interaction, basic residues for membrane stabilization through electrostatic interactions and scaffolding configuration induced by the Pro residue. Although curvature sensing behavior was observed for the monomeric Bradykinin peptide, stronger binding was observed for the trimeric form, suggesting how oligomerization may also play a role in curvature sensing behavior. Both of these studies exposed two different features that resulted in targeting highly curved vesicles, suggesting the complexity of this field and the need for further investigations to fully understand this behavior.

1.8 Project significance describing how MARCKS-ED targets highly curved membranes and nano-sized extracellular vesicles.

Our focus on membrane curvature and understanding protein-membrane interactions using peptides led us to identify the MARCKS-ED peptide as a curvature sensing peptide. In fact, MARCKS-ED has been observed to localize in cellular areas of positive curvature (*21*). It is also not so unexpected to observe curvature sensing behavior from a protein known to bind to phosphoinositol lipids as previously observed with other curvature sensing proteins (*1*). Our *in vitro* studies using synthetic lipid vesicles and *ex vivo* studies using secreted rat exosomes displayed this observation, which led us to further explore the biophysical interactions involved in MARCKS-ED's curvature sensing behavior. This could lead to identifying other curvature

sensing peptides for understanding protein-membrane interactions as well as targeting biological highly curved membranes such as shedding extracellular vesicles (EVs).

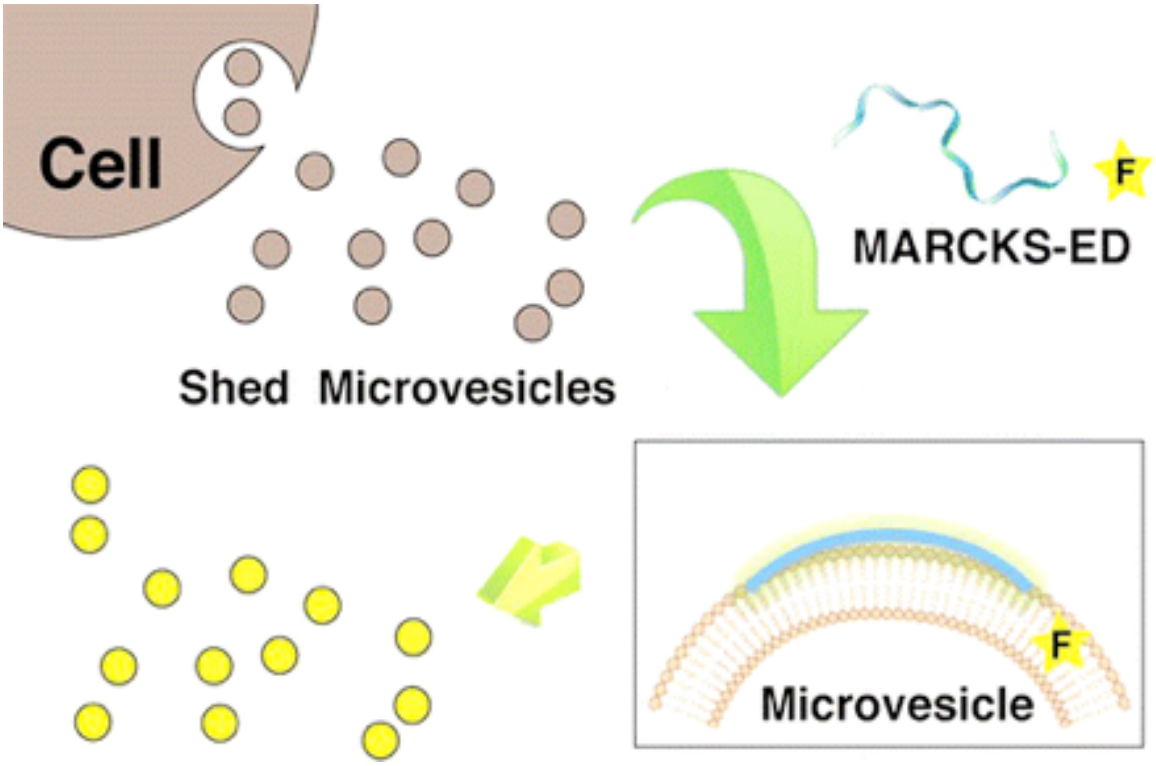

Scheme 1.4 Schematic of using peptides to target highly curved vesicles. The MARCKS-ED peptide is a natural peptide derived from the unstructured, cytoplasmic membrane protein myristoylated alanine-rich C-Kinase substrate (MARCKS) commonly known to interact with acidic lipids present on the inner leaflet of the plasma membrane using its effector domain (ED). Its curvature sensing behavior allows us to apply it to target highly curved vesicles for biophysical and biological applications. This figure is courtesy of Morton et al. (*22*).

CHAPTER 2

Designing a Protocol to Optimally Prepare and Extrude Different-Sized Vesicles using a Pressured Extruder.

Reformatted from the manuscript published under the same name of Constant Pressure-Controlled Extrusion Method for the Preparation of Nano-sized Liposomes in *J. Vis. Exp.* **2012**, *64*, e4151, co-authored with Saludes, J. P. and Yin, H.

2.1 Abstract.

Our studies involve analyzing and characterizing peptide-membrane interactions using a variety of methods for biophysical and biological applications. To further understand these interactions, we focus on performing *in vitro* experiments to measure binding. To isolate these peptide-membrane interactions on a molecular level, we use synthetic lipid components to create homogeneous solutions of lipid vesicles. This step is significant in our studies for measuring curvature sensing behavior of MARCKS-ED and other peptides using different lipid vesicle sizes. Membrane curvature studies are typically performed *in vitro* considering the complexities and experimental limitations associated with *in vivo* assays. Synthetically producing different sized lipid vesicles allows us to effectively study curvature sensing behavior, e.g. the binding preference that MARCKS-ED peptide has over different vesicle sizes. The lipid components used are based on a biologically relevant plasma membrane environment. This step is critical for our research because it strengthens our conclusions on what contributes to curvature sensing

behavior. So we designed a detailed protocol describing how to effectively generate distinct lipid vesicle sizes. We begin by describing how to prepare the lipid vesicle solution using an organic mixture followed by an extensive extrusion method to produce different vesicle sizes. We determine the accuracy of this pressurized-extrusion method through two characterization methods including dynamic light scattering (DLS) and nanoparticle tracking analysis (NTA) to measure and determine the specific vesicle diameter for each solution. These results show the importance of performing a developed extrusion method in order to produce different sized lipid vesicles, further providing support to our later conclusions on MARCKS-ED's preference for highly curved vesicles.

2.2 Introduction.

Liposomes are artificially prepared vesicles consisting of natural and synthetic phospholipids that are widely used as a cell membrane mimicking platform to study protein-protein and protein-lipid interactions (*3*), monitor drug delivery (*23, 24*), and encapsulation (*24*). Phospholipids naturally create curved lipid bilayers, distinguishing itself from a micelle (*25*). Liposomes are traditionally classified by size and number of bilayers, i.e. large unilamellar vesicles (LUVs), small unilamellar vesicles (SUVs) and multilamellar vesicles (MLVs) (*26*). In particular, the preparation of homogeneous liposomes of various sizes is important for studying membrane curvature which plays a vital role in cell signaling, endo- and exocytosis, membrane fusion, and protein trafficking (*27*). This protocol describes an extrusion method for preparing lipid vesicles of sub-micron sizes with a high degree of homogeneity. This method uses a

pressure-controlled system with controlled nitrogen flow rates for liposome preparation. The lipid preparation (*28, 29*), liposome extrusion, and size characterization will be presented herein.

Several groups analyze how proteins are used to modulate processes that involve membrane curvature and thus prepare liposomes of diameters <100 – 400 nm to study their behavior on cell functions (*3*). Others focus on liposome-drug encapsulation, studying liposomes as vehicles to carry and deliver a drug of interest (*30*). Drug encapsulation can be achieved as reported during liposome formation (*30*). Our extrusion step should not affect the encapsulated drug for two reasons, i.e. (a) drug encapsulation should be achieved prior to this step and (b) liposomes should retain their natural biophysical stability, securely carrying the drug in the aqueous core. These research goals further suggest the need for an optimized method to design stable sub-micron lipid vesicles. Nonetheless, the current liposome preparation technologies (sonication (*31*), freeze-and-thaw (*13*), sedimentation) do not allow preparation of liposomes with highly curved surface (i.e. diameter <100 nm) and with both high consistency and efficiency (*23, 31*), which limits the biophysical studies of an emerging field of membrane curvature sensing. Herein, we present a robust preparation method for a variety of biologically relevant liposomes.

Manual extrusion using gas-tight syringes and polycarbonate membranes (*23, 31*) is a common practice but heterogeneity is often observed when using pore sizes <100 nm due to inconsistency of pressure applied by the operator. We employed a constant pressure-controlled extrusion apparatus to prepare synthetic liposomes whose diameters range between 30 and 400

nm. Dynamic light scattering (DLS) (*31*), electron microscopy (*32*) and nanoparticle tracking analysis (NTA) (*13*) were used to quantify the liposome sizes as described in our protocol, with commercial polystyrene (PS) beads used as a calibration. A near linear correlation was observed between the employed pore sizes and the experimentally determined liposomes, indicating high fidelity of our pressure-controlled liposome preparation method. Further, we have shown that this lipid vesicle

preparation method is generally applicable, independent of various liposome sizes. Lastly, we have also demonstrated in a time course study that these prepared liposomes were stable for up to 16 hours. A representative nano-sized liposome preparation protocol is demonstrated below.

2.3 Experimental Methods.

Liposome preparation. A 20 mL glass vial with a Teflon-lined cap is retrieved and cleaned with chloroform prior to use to prevent contamination. Chloroform and methanol are transferred to the glass vials to produce an organic solution. Lipid components purchased by Avanti Polar Lipids are subsequently transferred into the glass vials at their respective volumes to create a 2 mM solution. The organic solvents are evaporated using slow-flow argon or nitrogen gas until a thin film of lipids is observed on the bottom of the vial. The uncapped glass vial is then placed in a vacuum dessicator for at least 30 minutes to remove residual solvent. Once a thin, white film is observed at the bottom of the glass vial, filtered PBS buffer is transferred to the vial to hydrate the lipids and produce lipid vesicles. The mixture is incubated over night at 4 °C and used within

48 hours.

Freeze-and-thaw for liposome sizes of 30-100 nm. To create unilamellar vesicles, the liposome suspension was frozen in liquid nitrogen for 15 seconds following overnight hydration. Using a heating block at 42 °C temperature, the liposome suspension was then thawed. This process was repeated for a total of 5 cycles.

Extrusion. The Avestin instructions describing how to correctly assemble the Liposofast LF-50 Extruder were followed using the instrument outline in their guidebook. The large hole support screen (with circular holes) was placed in the support filter base,
followed by the circular sintered dish (without holes), one drain disc (25 mm in
diameter), and one polycarbonate membrane (25 mm in diameter). The small, black O-ring was placed on top of the membrane to secure it to the support filter base. The top filter extruder was then attached by tightening 4 screws in the 4 corresponding holes. The filter extruder unit was assembled underneath the large extruder barrel. The liposome solution was added to the cylinder barrel. The following was placed on top of the extrusion barrel
in order: large circular O-ring, narrow cap, large circular O-ring, circular cap. The gas regulator was attached to the top of the extruder barrel top and all valves were closed to prevent any air leakage, including the pressure relief valve. A 20 mL glass vial or 50 mL Erlenmeyer flask was placed under the extruder filter unit. A safety valve is connected to the regulator and will release if pressure exceeds 600 psi. The nitrogen gas was turned on and the gas valve connected to the

extruder was opened. Increase The nitrogen pressure was increased to 25 psi for 400 nm liposomes, 125 psi for 100 nm liposomes, and 400-500 psi for 30 nm liposomes. The liposome suspension was observed as it ejected into the container while being pushed by the nitrogen. The nitrogen flowed until liquid was no longer observed passing through the extruder filter into the glass vial.

Dynamic light scattering (DLS). A 20 μM liposome solution was prepared. The power source and the lamp source were turned on prior to the start of the experiment. The DynaPro software was opened and set to the MS/X algorithm model to detect liposomes of 30 nm and 100 nm and MS800 algorithm model to detect >100 nm liposomes. The hardware was then connected. Liposome sample was pipetted into the quartz cuvette and inserted into the cell holder. Approximately 20 – 30 acquisitions were recorded. The average liposome diameter peaks were analyzed and recorded on the histogram.

Nanoparticle tracking analysis (NTA). A 500 μL, 0.1 μM liposome solution was prepared. The sample compartment was rinsed with water and ethanol. The sample compartment was then dried with a lint-free paper towel. The laser power source and the computer were turned on. A liposome solution of 300 μL, 0.1 μM was transferred to the sample compartment. The Temperature control and the Nanoparticle Tracking Analysis
software were opened. The capture button was pressed to turn on the laser.

Horizontal and vertical adjustments were made to move the stage and adjust the microscope focus. The desired temperature was set to 20 °C, and the recording time was set to 30 seconds. The record button was pressed to take multiple picture frames of the liposome particles for a specified amount of time. The peaks corresponding to the diameter liposome sizes were displayed on a histogram as it tracked the motion of each particle.

Negative stain Transmission electron microscopy (TEM). Carbon Formvar mesh grids were negatively discharged prior to sample staining, where 1% Uranyl acetate in water was used to stain the samples prior to drying and imaging at 34,000x magnification.

2.4 Results.

A scheme outlining the extrusion method is presented in Figure 2.1. To obtain optimum results, preparation of liposomes with diameters of 30 nm requires a high pressure of ~ 500 psi and diameters of 100 nm requires a pressure of 125 psi to achieve a rapid filter rate. For diameters of 400 nm, a low pressure of ~ 25 psi is recommended to achieve a slower filter rate, which allows the vesicles to elongate and form larger, homogeneous liposomes. We conducted a series of experiments to determine the optimal pressure for producing consistent sub-micron vesicle sizes. We varied the pressure as well as the number of extrusion passes through polycarbonate filters with pore sizes of 30, 100, and 400 nm and discovered appropriate pressure for each desired size. For 30 nm pores, pressure below 500 psi will reduce the flow rate, causing elongation and

thus larger vesicle sizes. For 100 nm pores, a steady flow was achieved at 125 psi. For 400 nm pores, low pressure (25 psi) allows the vesicles to elongate into larger vesicle sizes. A slow drop-wise filtration flow is optimal to create larger sub-micron vesicles (*33*).

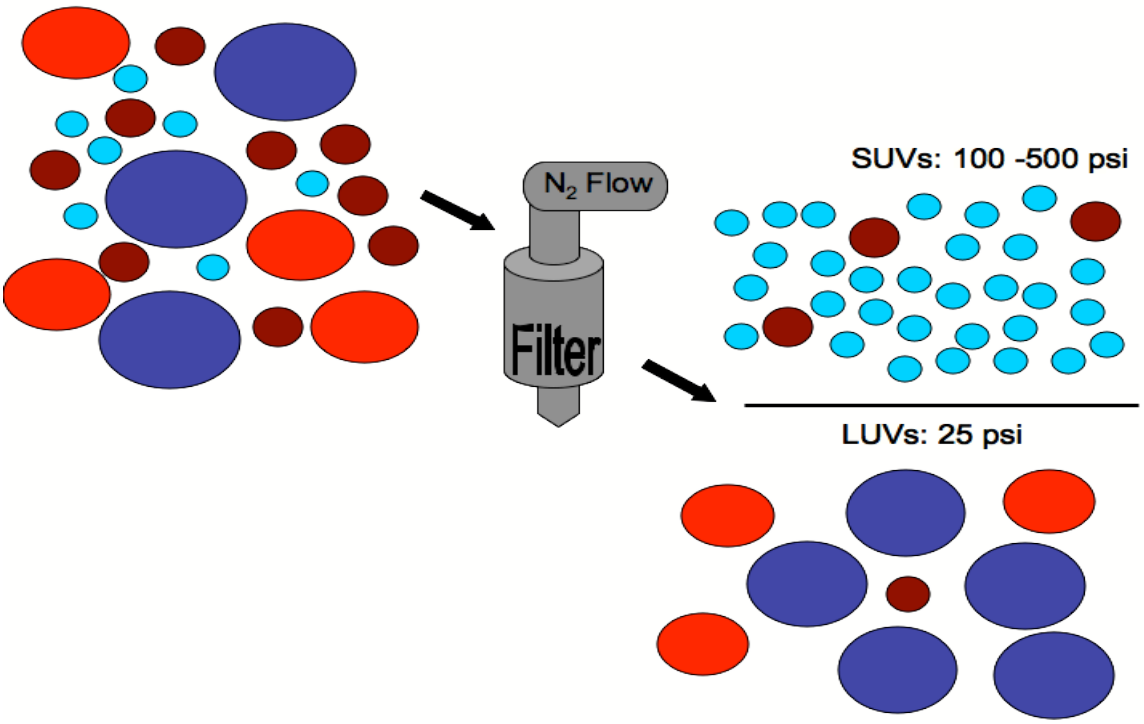

Figure 2.1 Flow chart of the extrusion method, describing how the pressure and nitrogen flow controls the homogeneity of different liposome diameters. Following liposome hydration,

unilamellar vesicles of different sizes are extruded through different polycarbonate membrane filter pores at different pressures (*34*). Courtesy of Morton et al (*34*).

We performed DLS to determine the liposome sizes extruded through three different diameter sizes, i.e. 30, 100 and 400 nm. DLS is an established method that collects scattered light to determine the particle diameter. We extruded hydrated liposomes of 2 mM through a polycarbonate 30 nm membrane at 500 psi with 5 passes through the filter pore; a 100 nm polycarbonate membrane at 125 psi with 5 passes through the filter pore and a 400 nm polycarbonate membrane at 25 psi with 2 passes through the filter pore. The diameters of the liposomes and measured by DLS for 30, 100 and 400 nm pore sizes were 66 ± 28, 138 ±18 and 360 ± 25 nm (Figure 2.2). A suspension of 50 nm polystyrene beads was used as a calibration standard as shown in Figure 2.2, where it recorded a diameter of 47 ± 16 nm. The percent polydispersity shows that there is no overlap within liposome sizes. It is typical to observe diameters higher than 30 nm when using DLS analysis due to the known bias this instrument has towards larger particles (*13*). Light scatter intensities from large and small particles are collected simultaneously from one detection method and thus harder to resolve liposomes in suspension (*13*). Despite this instrumental limitation, the calibration curve describes a near linear correlation.

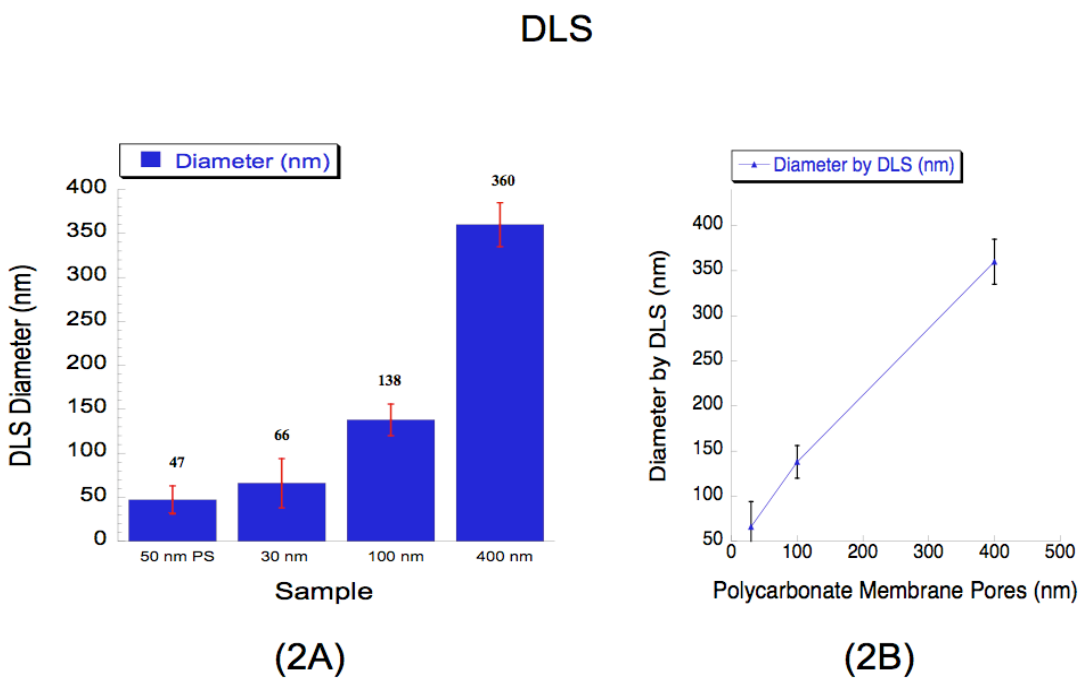

Figure 2.2 Dynamic Light Scattering (DLS) data describing the quantitative liposome sizes following extrusion. (a) Bar graphs are shown to describe the diameters of the three-liposome samples. A calibration standard of 50 nm polystyrene (PS) beads was used as a reference. The average liposome diameters are indicated above the bar for each sample. The x-axis describes the pore sizes of which the solutions were extruded through. The y-axis describes the diameter recorded by DLS. Although the 30 nm and 100 nm sizes recorded values higher than their pore sizes while the larger 400 nm size recorded a slightly lower size, the calibration curve (b) shows a near linear correlation, where the x-axis expresses the polycarbonate membrane pore sizes, and the y-axis describes the recorded liposome diameter by DLS (*34*). Courtesy of Morton et al (*34*).

NTA is a new technology that measures the size of each particle from direct observations of diffusion in a liquid medium, independent of particle refractive index or density. This high-resolution technique can be used to supplement the measurement of liposomes with DLS. The NTA recorded diameters of 95 ± 48 and 356 ± 51 nm, two 100 nm and 400 nm polystyrene solutions were used for calibration. Lipid solutions of 30 nm and 100 nm were observed to have a more comparable diameter relative to the DLS as shown in Figure 2.3, producing average sizes of 29 ± 14, 95 ± 17 and 359 ± 73 nm. The NTA may be a more general characterization technique to quantify microscopic particles since its sensitivity allows it to measure particles of 50 – 1000 nm. The calibration curve shows a linear correlation between the polycarbonate membrane pores versus the recorded NTA diameter.

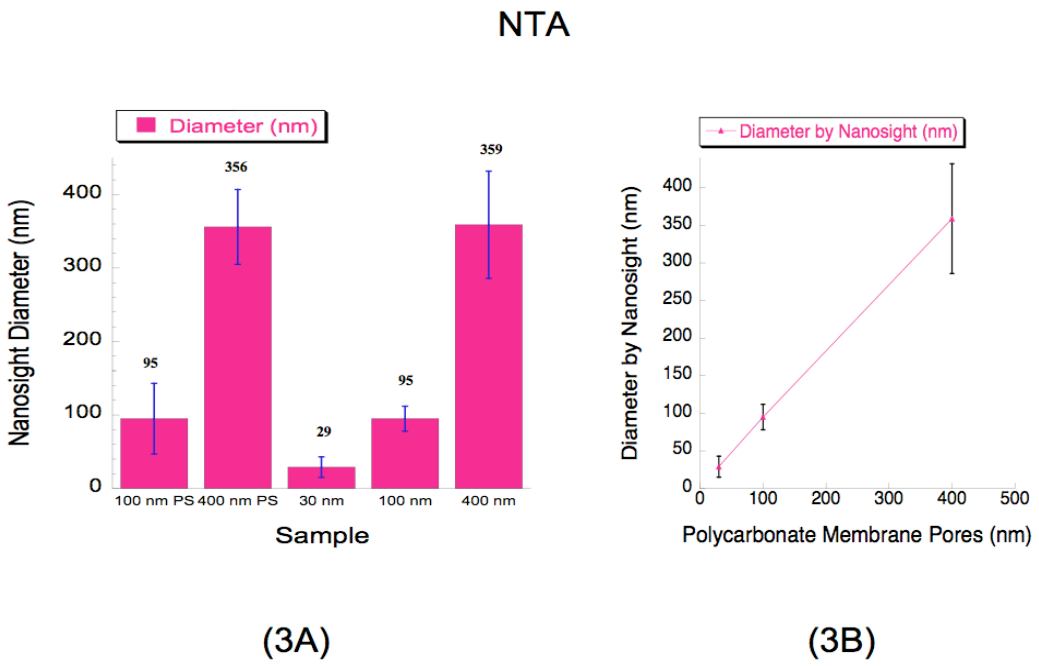

Figure 2.3 Nanoparticle Tracking Analysis (NTA) data describing the liposome sizes following extrusion. (a) The bar graphs represent the diameter of each liposome sample. The x-axis describes the pore sizes of which the solutions were extruded through. The y-axis describes the size diameter recorded by the NTA. The average liposome diameters are labeled above each sample. (b) The NTA calibration curve shows a more linear correlation than the DLS calibration curve between the filter membrane pore sizes versus the recorded diameter. The x-axis describes the polycarbonate membrane pore sizes. The y-axis describes the recorded liposome diameter by NTA (*34*). Courtesy of Morton et al (*34*).

Negative stain transmission electron microscopy was performed to visually observe the stability and morphology of the prepared liposomes following extrusion. This method was performed to further confirm different sizes that were generated for biophysical and biological studies. This particular technique was performed based on previous reports that have carried out TEM for lipid vesicle characterization (*3*). As shown in Figure 2.4, three lipid vesicle sizes were stained, observed and recorded.

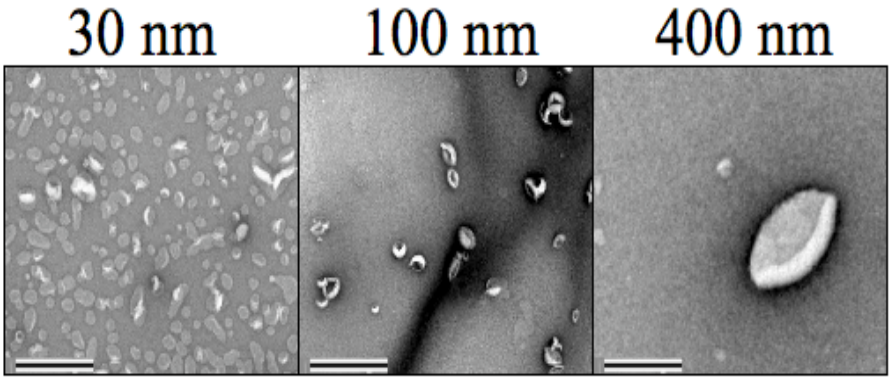

Figure 2.4 Negative stain transmission electron microscopy (TEM) images. These images show each liposome size (500 μM) followed by extrusion. Sizes 30, 100, and 400 nm are clearly distinct from each other. The magnification was set to 25,000x. The scale bar represents 0.5 μm (*34*).

To determine the stability of our generated liposomes, we conducted dynamic light scattering (DLS) and performed an overnight time-course experiment. The vesicle diameter was

measured for each liposome solution immediately following extrusion. All liposome solutions were stored in 4ºC overnight. Their diameters were recorded again by the DLS after an overnight incubation. As shown in Figure 2.5, negligible to no change in liposome diameter was recorded following an overnight incubation period.

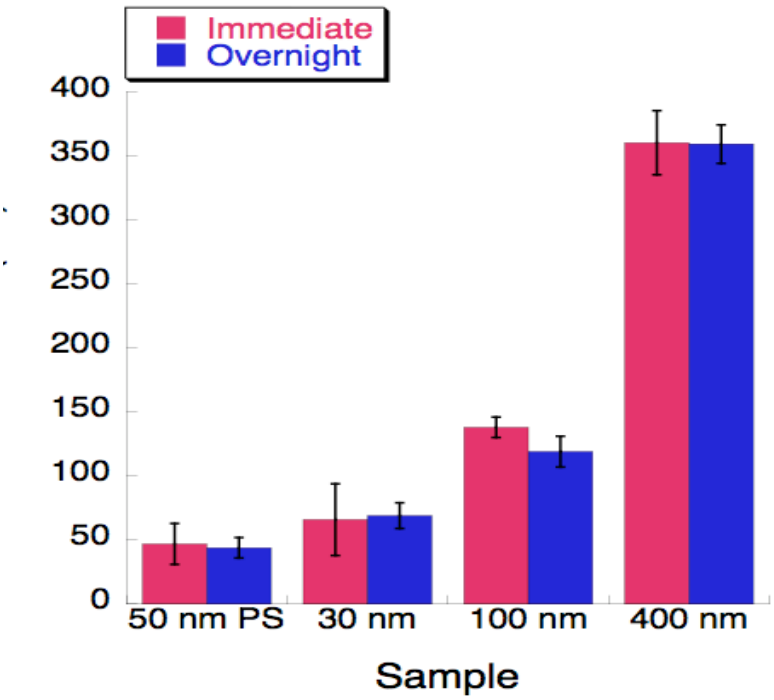

Figure 2.5 A time-course experiment was conducted with three liposome sizes. Little to no change was observed after a 16-hour incubation period (*34*).

2.5 Discussion.

Using the Avestin Liposofast LF-50 Extruder, we demonstrated how small-sized, synthetic liposomes are prepared through a pressure-controlled system. It is important to note

that multilamellar vesicles form spontaneously following liposome hydration, which may lead to production of smaller nanoparticles. These small multilamellar vesicles will inevitably flow through the larger polycarbonate membrane pore size, causing heterogeneity in solutions of unilamellar vesicles produced by a large filter pore. Therefore, it is recommended to reduce the nitrogen flow pressure when large pore sizes are used (i.e. 25 psi for 400 nm diameter pores as described above) in order to give the lipids sufficient time to fuse and elongate into larger vesicles, increasing the homogeneity of the solution. For liposomes with diameters of <100 nm, high pressure (i.e 400-500 psi for 30 and 100 nm as described above) is applied for a rapid extrusion to increase lipid trapping efficiency and size homogeneity.

A few notable steps are recommended to ensure accurate, reproducible liposome preparation. It is best to prepare vesicles with the minimum volume of 3.0 mL of sample for extrusion using the described method. Samples with lipid concentrations above 2 mM will require higher nitrogen pressure of > 500 psi for diameters <100 nm, which should be conducted with caution considering that such pressure is beyond the instrumental upper limit. A recommendation of repetitive passes (5~7 reiterations) through the extruder filter will improve the vesicle solution homogeneity. Using glass vials and syringes for sample preparation will prevent any leaching from polypropylene tubes that could contaminate the liposome sample. It is also critical to filter the resultant liposomes to remove any possible residual dust particles.

In the method described above, we have employed two methods to characterize liposome sizes, namely DLS and NTA. Both techniques showed a near linear correlation between the pore

sizes versus the actual observed liposome diameter. Nonetheless, one should bear in mind that a statistically significant, but unsubstantial heterogeneity of lipid vesicles was observed using both characterization methods. In summary, we have described a well-controlled method for producing nano-sized synthetic liposomes with high consistency and efficiency.

CHAPTER 3

MARCKS-ED Peptide as a Curvature and Lipid Sensor

Manuscript published under the same name in *ACS Chem. Biol.* **2013**, *8*, 218-225, co-authored with Saludes, J.; Fiorini, Z.; Beninson, L.; Chapman, E.; Fleshner, M.; Xue, D. and Yin, H.

3.1 Abstract.

Membrane curvature and lipid composition regulates important biological processes within a cell. Currently, several proteins have been reported to sense and/or induce membrane curvatures, e.g., Synaptotagmin-1 and Amphiphysin. However, the large protein scaffold of these curvature sensors limits their applications in complex biological systems. Our interest focuses on identifying and designing peptides that can sense membrane curvature based on established elements observed in natural curvature-sensing proteins. Membrane curvature remodeling also depends on their lipid composition, suggesting strategies to specifically target membrane shape and lipid components simultaneously. We have successfully identified a 25-mer peptide, MARCKS-ED, based on the effector domain sequence of the intracellular membrane protein myristoylated alanine-rich C-kinase substrate that can recognize PS with preferences for highly curved vesicles in a sequence-specific manner. These studies further contribute to the understanding of how proteins and peptides sense membrane curvature, as well as provide potential probes for membrane shape and lipid composition.

3.2 Introduction.

Membrane curvature plays a vital role in cell signaling, endo- and exocytosis, membrane fusion, and protein trafficking (*27*). Naturally occurring proteins with a Bin-Amphiphysin-Rvs domain or with the ArfGAP1 Lipid Packing Sensor (ALPS) motif are known to be able to sense membrane curvature (*7, 35*). However, these large proteins are not optimal for large-scale production, limiting their uses in biotechnology developments. Our primary goal is to identify peptides with curvature-sensing ability that can potentially be used for extracellular vesicle detection based on shape and lipid composition. Herein, we report a short peptide derived from the effector domain of myristoylated alanine-rich C-kinase substrate (MARCKS-ED) that selectively recognizes highly curved membrane surfaces. MARCKS-ED preferentially binds to highly curved surfaces of both synthetic lipid vesicles and isolated extracellular vesicles in rat blood plasma. Furthermore, we also observed that the MARCKS-ED peptide recognizes vesicle surfaces based not only on size but also on their lipid component, detecting the negatively charged phosphatidylserine (PS) exposed on the cell surface of a *C. elegans* animal model. These results demonstrated that MARCKS-ED recognizes PS lipid composition and membrane curvature, shedding insight into the understanding of protein−lipid interactions in curvature sensing.

MARCKS is an 87-kDa intracellular protein whose functions involve sequestering phosphatidylinositol 4,5-bisphosphate (PIP_2) and regulating Phospholipase C signaling (*36*). The MARCKS protein also recognizes PS, the negatively charged lipid enriched on the inner leaflet of the cytoplasmic membrane, using its ED (aa 151−175) region (*14*). This protein−membrane

association can be regulated and reversed by its binding to Calmodulin (CaM) in the presence of Ca^{2+} (*19*).

We focused on the ED region of the MARCKS protein in our search for curvature-sensing peptides based on the following rationales: First, it has been established that the membrane binding by the MARCKS protein is driven by electrostatic interactions between the cationic residues (i.e., Lys, Arg) within the ED peptide region and PS, while the secondary structure is not important (*37*). This suggests that the unfolded, truncated MARCKS-ED peptide may still retain the membrane binding ability of the full-length protein. Second, curved membranes are known to expose more phospholipid packing defects at the membrane surface due to the asymmetric stretching of the bilayer (*38*). Previous studies have shown that the BAR domains sense curvature partially by detecting these lipid packing defects (*7*). The MARCKS protein was reported to insert the aromatic side chains of five Phe residues from the ED region into the lipid bilayers (*20*). We hypothesized that such insertion could in turn stabilize the membrane defects of highly curved vesicles. This hypothesis is consistent with the previous observation that MARCKS is localized in areas of the cell membrane with positive curvature (*21*).

3.3 Experimental Methods.

Solid Phase Peptide Synthesis. Peptides were synthesized using a CEM Liberty microwave-assisted peptide synthesizer following the standard solid phase Fmoc chemistry (*39*). For fluorophore labeling, 4- chloro-7-nitrobenzo-2-oxa-1,3-diazole (NBD) or Alexa Fluor 546 was conjugated to the N-terminus of the peptide via a flexible linker, ε-aminohexanoic acid, using the

previously reported coupling method (*39*). A Kaiser test was performed to confirm the efficiency of the fluorophore labeling (*40*). Following purification, peptides were lyophilized to produce a TFA salt powder. The prepared peptides were characterized by matrix-assisted laser-desorption ionization time-of-flight (MALDI) to confirm their identity.

Synthetic Lipid Vesicle Preparation. To produce various lipid vesicles, we followed a previously established protocol (*34*). The phospholipids 1-palmitoyl-2-oleoyl-sn-glycero-3-phosphoethanolamine (POPE), 1-palmitoyl-2-oleoyl-sn-glycero-3-phospho-L-serine (POPS), 1-palmitoyl-2-oleoyl-sn-glycero-3-phosphocholine (POPC), and cholesterol (Avanti Lipids) were mixed at the appropriate amounts to produce stock solutions for all synthetic lipid models, using lipids present in physiological membranes (*41*). For Annexin-V fluorescence enhancement studies, sphingomyelin and phosphatidylinositol were added to mimic the *C. elegans* outer leaflet membrane (*42*).

Circular Dichroism (CD) Spectroscopy. The peptide solutions were prepared at 10 μM in 10 mM phosphate buffer (pH = 7.40) in\ the presence of 500 μM lipid vesicles (30 nm pore size with 20% PS). Circular dichroism spectra were recorded using a Chirascan CD spectrometer (Applied Photophysics) with a 1 mm path length quartz cuvette at 20 °C using phosphate buffer as a blank. The reading was then converted to molar residue ellipticity (θ). Five scans from 190 to 260 nm with data points taken every 1.0 nm were obtained and averaged for each sample.

Cosedimentation Assay. MARCKS-ED (10 μM) was incubated with 600 μM synthetic vesicles of sizes 100 and 400 nm. The positive control was the intact C2A-C2B cytoplasmic domains (C2AB) of rat Synaptotamin-1 (aa 96−421). C2AB (1.5 μM) was treated with CaCl2 (1 mM) and incubated with 300 μM synthetic vesicles of sizes 100 and 400 nm, based on the vesicle concentrations previously reported.16 C2AB treated with vesicles was incubated at RT for 30 min, followed by centrifugation of 65,000 rpm for 45 min at 20 °C. MARCKS-ED treated with vesicles was incubated at RT for 2 h, followed by 75,000 rpm for 45 min at 20 °C. The supernatant for each sample was
collected as well as the pellets from the MARCKS-ED-treated samples and assayed on a precasted 12−15% Tris-Bis gel (Invitrogen).

Fluorescence Enhancement Assay. The emission spectra of all NBD-labeled peptides were recorded using a Fluorolog-3 fluorometer (Horiba Jobin Yvon) with λ_{ex} = 480 nm. The peptides and protein were tested at a concentration of 500 nM in PBS (pH = 7.40) treated with 500 μM synthetic vesicles of different vesicles sizes. Fluorescence was observed with an emission range of 500−650 nm. Monitored at λ_{ex} = 295 nm, Annexin-V (0.32 μM) was treated with $CaCl_2$ (3 mM) in TES buffer and with 500 μM lipid vesicles of varying PS content. An emission spectrum of 300−450 nm was recorded. The positive control C2AB (200 nM) from the rat Synaptotagmin-1 (Syn-1) protein (G374, residues 96−421) was treated with $CaCl_2$ (2.5 mM) and observed with λ_{ex} of 275 nm and emission range of 300−450 nm. The untreated peptide and Ca^{2+}-C2AB

samples were corrected by the PBS (pH = 7.40) blank solution for the peptides and PBS with Ca^{2+} for the Ca^{2+}-C2AB sample. All samples were prepared and incubated overnight in 4 °C.

Fluorescence Anisotropy Assay. The NBD-labeled peptides (1 μM) were titrated by synthetic liposomes of various sizes (30, 100, and 400 nm). Fluorescence anisotropy was recorded using a Fluorolog-3 fluorometer. The mixture was allowed to equilibrate for 2 min prior to the next titration. The excitation wavelength was set to λ_{ex} = 480 nm whereas the emission filter was set to λ_{em} = 545 nm. The voltage was set to 250 V throughout the experiment. Blank PBS (pH= 7.40) was titrated to NBD-labeled peptides as a negative control, where negligible anisotropy change was observed.

Microvesicle Preparation. Adult male Fisher 344 rats (Harlan, 8−9 weeks old) weighing approximately 250−275 g were used in all experiments. Animals were singly housed in clear Nalgene plastic cages (48 °— 27 °— 20 cm) and allowed access to food and water ad libitum. Temperature and humidity remained constant and animals were
maintained on a 12-h:12-h light-dark cycle (lights on at 7:00 a.m.). Animals were allowed to acclimate to these housing conditions for 1 week prior to any experimental manipulations and were handled each day. The care and treatment of the animals were in accordance with protocols approved by the University of Colorado Institutional Animal
Care and Use Committee. An in-house exosome assay based on a reported ELISA method22 was used for two common markers of exosomes, the tetraspanin CD63 and the membrane transport

protein Rab5b. Particles expressing both proteins were captured by antibodies and quantified in a colorimetric end point assay.

Nanoparticle Tracking Analysis. Nanoparticle tracking analyses were performed using the NanoSight LM10-HS instrument equipped with a 532 nm laser and observed at scatter and fluorescence modes (filter = 550 nm). The instrument was calibrated using commercially available 50-nm polystyrene beads (Polysciences). Parallel experiments were done on isolated exosomes and plasma that were not treated with MARCKS-ED conjugated with Alexa Fluor 546 to confirm that the suspended particles do not autofluoresce. Alexa Fluor 546-labeled mouse anti-rat CD63 (AbD Serotec) and unconjugated Alexa Fluor 546 were used as positive and negative controls, respectively. The profiles of MARCKS-ED-Alexa Fluor 546 and Alexa Fluor 546 in the absence of microvesicles were also investigated to confirm that these show negligible scatter and fluorescence background signals under identical NTA conditions.

***In Vivo* Staining of *C. elegans* Gonads.** Gonads of wild type (N2), tat-1(tm3117), or ced-7(n2094) *C. elegans* animals were stained as previously described.25 Briefly, 36-h-old hermaphrodite adult animals were collected and gently dissected by cutting their heads in a depression slide with a gonad dissection buffer (60 mM NaCl, 32 mM KCl, 3 mM Na_2HPO_4, 2 mM $MgCl_2$, 20 mM HEPES, 50 μgmL−1 penicillin, 50 μg mL−1 streptomycin, 100 μg mL−1 neomycin, 10 mM glucose, 33% fetal calf serum, and 2 mM $CaCl_2$) to expose the gonads. The exposed gonads were then washed once in the dissection buffer and transferred to a dissection

buffer containing 4 μM Hoechst 33342 and 20 μM NBD labeled MARCKS-ED peptide, 20 μM NBD labeled MARCKSmut1 peptide, or 10 nM Alexa Fluor 488-conjugated Annexin-V for 45 min. Gonads were washed one more time in the dissection buffer, placed on a 5% agarose pad, and visualized using a Nomarski microscope equipped with an epifluorescence detector.

3.4 Results.

The MARCKS-ED peptide (Table 3.1) was synthesized using standard microwave-assisted solid phase Fmoc chemistry. To MARCKS peptides were prepared: (i) the five Phe residues that have been previously suggested to vertically insert into the bilayers were mutated to Ala to generate MARCKSmut1, and (ii) the positively charged residues (Lys, Arg) were mutated to Ala to generate MARCKSmut2. We also synthesized MARCKS-ED-scr with a scrambled sequence to investigate the sequence specificity of MARCKS-ED. Fluorescently labeled MARCKS-ED, MARCKSmut1, MARCKSmut2, and MARCKS-ED-scr peptides were prepared by conjugating either NBD or Alexa Fluor 546 to their N-termini via a flexible ε-aminohexanoic acid linker. To observe the secondary structure of MARCKS-ED, circular dichroism (CD) analysis was performed for both untreated and vesicle-treated peptide. In agreement with previous reports (*43, 44*), MARCKS-ED does not demonstrate any predominant secondary structures (Supplementary Figure 1) in aqueous solution. In the presence of lipid vesicles, its CD spectrum did not differ significantly, suggesting that MARCKS-ED remains primarily unstructured.

MARCKS-ED:	KKKKKRFSFKKSFKLSGFSFKKNKK
MARCKSmut1:	KKKKKRASAKKSAKLSGASAKKNKK
MARCKSmut2:	AAAAAAFSFAASFALSGFSFAANAA
MARCKS-ED-scr:	KKKGKKNSSKKFFFFSKFKLSRKKK

Table 3.1 List of synthesized MARCKS-ED peptides. Cationic residues critical for the electrostatic interactions with PS are highlighted in red. The Phe residues speculated to stabilize the curvature defects are shown in blue.

We first prepared synthetic vesicles of various sizes (diameter ϕ = 30, 100, and 400 nm) and with various lipid compositions (Supplementary Figure 2) that closely resemble the lipid composition of biological membranes (*41*). Dynamic light scattering (Supplementary Figure 3) and negative-stain transmission electron microscopy (TEM) (Supplementary Figure 4) were used to validate the lipid vesicle sizes with commercial polystyrene beads as the calibration standard. Furthermore, a time-course experiment was carried out to confirm the stability of the vesicles up to 16 h (Supplementary Figure 3).

A previously established cosedimentation assay was performed to test the curvature sensing behavior of MARCKS-ED (*45*). Two vesicle pore sizes, 100 and 400 nm, were used in this experiment because vesicles smaller than 100 nm were difficult to pellet even at high centrifugation speed. We also used a previously reported curvature sensing protein, C2AB, as a positive control (*3*). Figure 3.1 shows the gel electrophoresis results of the supernatant and pellet samples collected after sedimentation with MARCKS-ED or C2AB, respectively. A reduction in band intensity indicates that more MARCKS-ED or C2AB was pulled down by the 100 nm PS-containing vesicles than by the larger 400 nm vesicles. Also, less MARCKSED was pulled down

by the lipid vesicles without PS, suggesting that both the peptide-lipid binding and its curvature sensing depend on the presence of PS. Taken together, these results showed that, similarly to the C2AB protein, MARCKSED preferentially binds to highly curved vesicles containing PS.

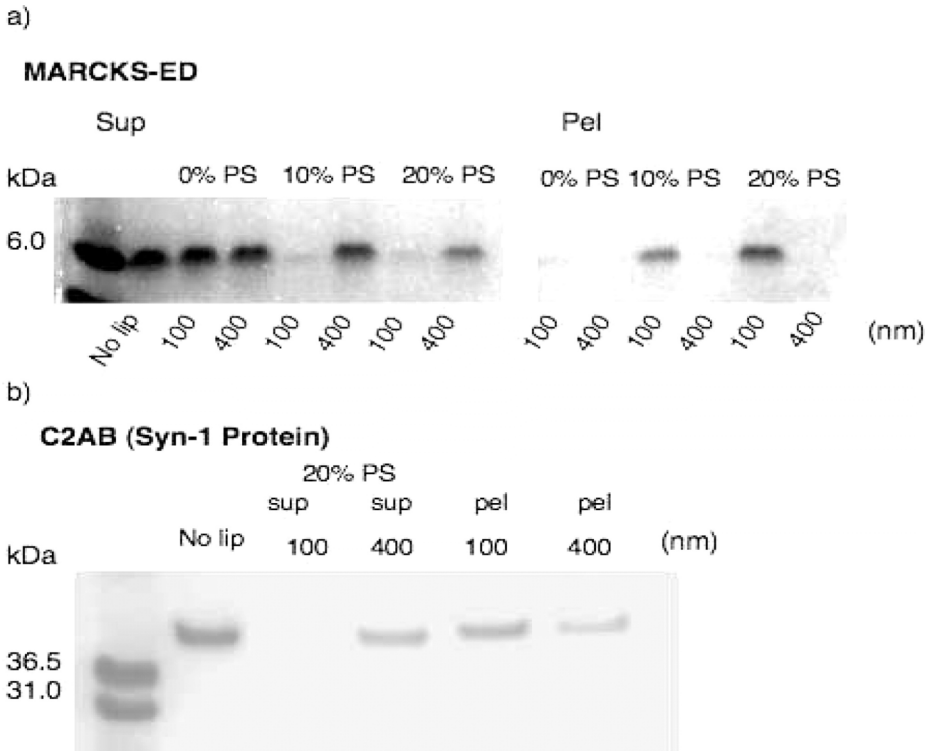

Figure 3.1 Cosedimentation pull-down assay. SDS gel of synthetic liposomes of different sizes with (a) MARCKS-ED or (b) the curvature-sensing C2AB domain of Synatptotagmin-1. Sup = supernatant. Pel = pellet. No lip = no lipid vesicles. [C2AB] = 1.5 μM. [Ca^{2+}] for C2AB only = 1 mM. [MARCKS-ED] = 10 μM. [Lipid $Vesicle_{C2AB}$] = 300 μM. [Lipid $Vesicle_{MARCKS\text{-}ED}$] = 600 μM.

Next, we conducted a fluorescence enhancement assay to further validate the curvature- and PS-sensing behavior of MARCKS-ED. Upon binding to lipid vesicles of different sizes and lipid compositions, the fluorescence intensity of the NBD-labeled MARCKS-ED peptide increased due to the elevated hydrophobicity of the surrounding environment of the fluorophore (Supplementary Figure 5). Figure 3.2a shows that the fluorescence enhancement of MARCKS-ED treated with the 30 nm pore size lipid vesicles containing PS is significantly higher than the samples treated with both the 100 and 400 nm vesicles (statistic analysis was carried out using the ANOVA method, Supplementary Tables 2, 3, and 4). Appropriate controls were performed to confirm that the fluorophore alone has no effect on the observed fluorescence enhancement (Supplementary Figure 6a and b). Compared to the samples treated with the 400 nm vesicles, samples treated with the 30 nm vesicles showed a fluorescence intensity increase of approximately 1.5-fold, a change that is greater than the ones induced by the positive control protein, C2AB (Supplementary Figure 6c). MARCKS-ED-scr also showed a binding preference to highly curved vesicles containing 10% PS (Figure 3.2b) butnot to vesicles containing 0% or 20% PS (Supplementary Figure 7). The fluorescence intensity enhancement by MARCKS-ED-scr, however, is remarkably lower at all of these different PS concentrations. MARCKSmut1 and MARCKSmut2 both showed significantly reduced fluorescence enhancement and lacked the curvature sensing behavior observed in the wild type MARCKS-ED (Figure 2b, Supplementary Figure 8). Furthermore, the specificity of MARCKS-ED was confirmed by the observation that its binding can be partially reversed by the addition of CaM (Supplementary Figure 6d), which is in agreement with the behavior of the full-length MARCKS protein. Lastly, the

fluorescence intensity differences were less significant with vesicles containing no PS. Taken together, we concluded that MARCKS-ED recognizes PS with a preference for highly curved vesicles in a sequence-specific manner.

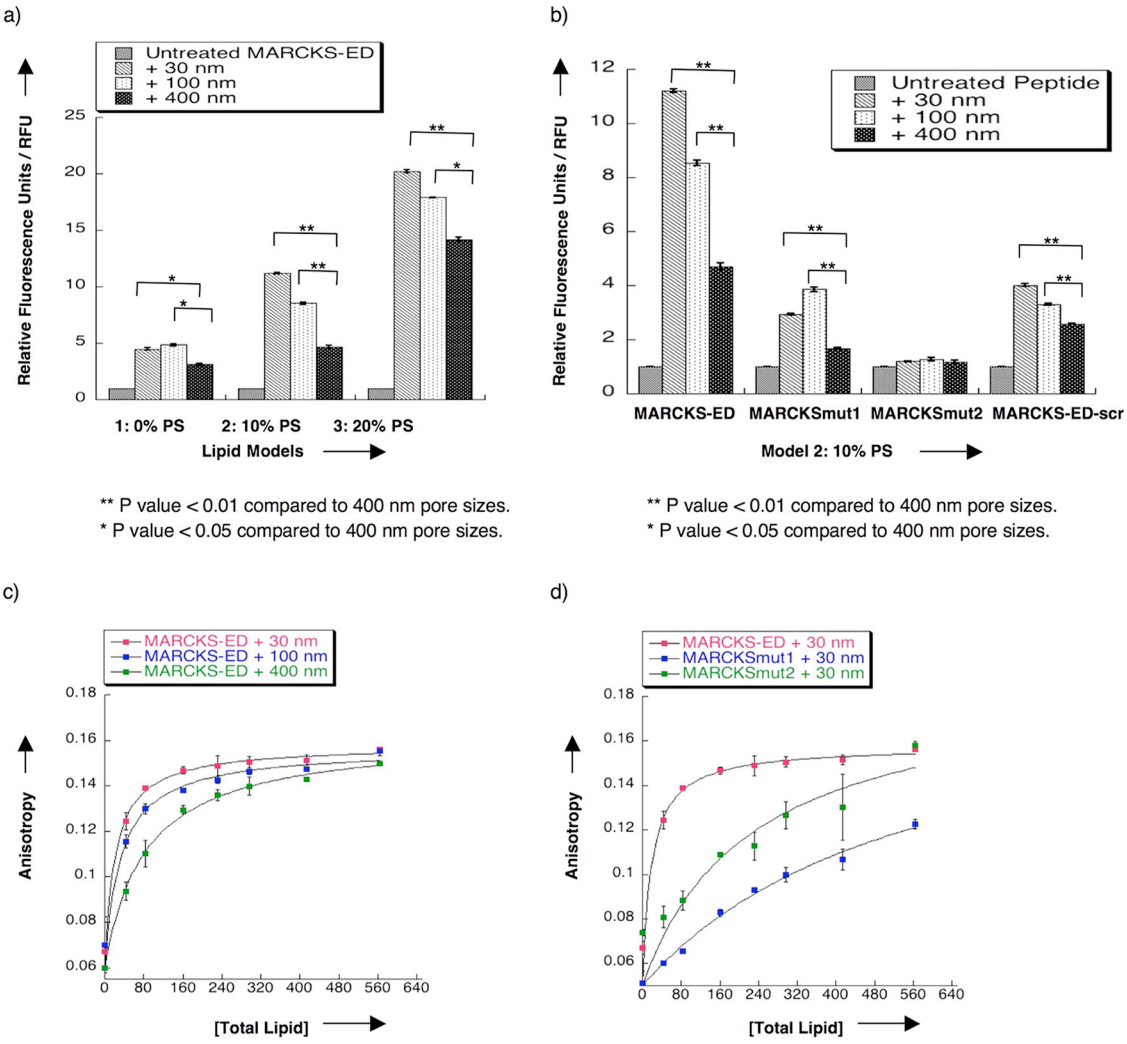

Figure 3.2 Fluorescence enhancement assay. Bar plots (a and b) with the NBD label attached to the N-terminus *via* a flexible ε-aminohexanoic acid linker to MARCKS-ED, MARCKSmut1, MARCKSmut2, and MARCKS-ED-scr. [Peptide] = 500 nM. [Total Lipid] = 500 μM. The *y*-axis

is described in relative fluorescence units (RFU). Fluorescence was normalized to the untreated NBD-MARCKS-ED peptide samples (RFU = 1). (a) Bar graphs showing greater fluorescence of MARCKS-ED treated with 30 nm lipid vesicles containing PS. (b) Bar graphs showing reduced binding and curvature-sensing behavior with mutant peptides, MARCKSmut1, MARCKSmut2 and MARCKS-ED-scr, with lipid vesicles containing 60% POPC:15% cholesterol:15% POPE:10% POPS. ***P* value < 0.01 compared to 400 nm pore sizes. **P* value < 0.05 compared to 400 nm pore sizes. (c) Fluorescence anisotropy titration of MARCKS-ED with various sized lipid vesicles containing 60% POPC:15% cholesterol:15% POPE:10% POPS. (d) Fluorescence anisotropy titration of various MARCKS peptides with 30 nm pore size lipid vesicles containing 60% POPC:15% cholesterol:15% POPE:10% POPS. The plots were fitted using a standard one-site saturation equation (*15*). [Peptide] = 1 μM. Phosphate-buffered saline (PBS, pH = 7.4) buffer was used in all sample preparation.

Because fluorescence enhancement assays could not distinguish the contributions between different degrees of membrane penetration and binding affinity, we performed a fluorescence anisotropy assay to specifically measure the binding affinity of the MARCKS peptides. Lipid vesicles were titrated to NBD-labeled MARCKS-ED, MARCKSmut1, or MARCKSmut2 peptides. Since the peptide partitions between the hydrophobic lipid bilayer and the aqueous solvent, the molar partition coefficient (K_p) is often reported (*43*). By definition, the apparent dissociation constant (K_D), described as the lipid concentration where 50% of the

peptide is bound, is the reciprocal of the molar partition coefficient (*15*). Our results indicated that MARCKS-ED binds more tightly to highly curved vesicles. As shown in Figure 3.2c and Supplementary Figure 9, MARCKS-ED was found to bind to 30, 100, and 400 nm pore size lipid vesicles containing 10% PS with Kd values of 24 ± 3, 42 ± 13, and 86 ± 20 μM, respectively. As a comparison, C2AB showed a 1.9-fold increase in binding to smaller vesicles (105 nm) relative to the larger ones (252 nm) (*3*). Statistical analysis was performed using ANOVA single factor analysis (Supplementary Tables 5 and 6). By contrast, MARCKSmut1 showed a reduced binding affinity (Figure 3.2d), confirming the critical roles of the Phe residues (*21*). Similarly, electrostatic interactions also contribute importantly to the binding affinity as MARCKSmut2 is observed to have a weaker binding affinity. These data suggest that both aromatic and cationic residues are required for MARCKS-ED, which is in agreement with our speculation that the interactions between MARCKS-ED and small, PS-enriched vesicles are driven by both electrostatic interactions and the inserted Phe residues that presumably stabilize defects of curved bilayers.

Having established the simultaneous curvature- and PS-sensing by MARCKS-ED in synthetic lipid vesicles, we investigated if MARCKS-ED could detect highly curved, PS-enriched extracellular particles (e.g., microvesicles and exosomes) in a complex biological system. Microvesicles (ϕ = 0.1−1 μm) and exosomes (ϕ = 0.03−0.1 μm) are highly curved lipid vesicles that are shed into bodily fluids (e.g., blood, urine, ascitic fluid) (*46*). They are released by stressed or cancerous cells in which lipid asymmetry is deregulated, thus resulting in the externalization and enrichment of PS on their outer leaflet (*12*). A direct correlation between the

overexpression of these extracellular vesicles in the blood and cancer metastasis has been observed in B16 mouse melanoma cells (*9*). We investigated if MARCKS-ED could detect extracellular vesicles using plasma samples from a stressed rat model (*47*). The extracellular vesicles in these samples were characterized by TEM imaging (Supplementary Figure 10a) and immunoblot analysis of the signature CD63 protein exposed on the surface of exosomes and microvesicles (Supplementary Figure 10b) (*47*). These nanosized, isolated vesicles were measured by nanoparticle tracking analysis with an average size of ϕ = 56 nm. Lastly, we also confirmed any exposed PS on their membrane surface with an established PS-sensing protein, Annexin-V. Previous reports showed that upon binding to PS-enriched synthetic lipid vesicles, the fluorescence from W187 of Annexin-V would increase (*48*). Indeed, fluorescence enhancement was observed for the Annexin-V protein incubated with the isolated extracellular vesicles from our tested animal models, indicating specific PS recognition (Figure 3.3a).

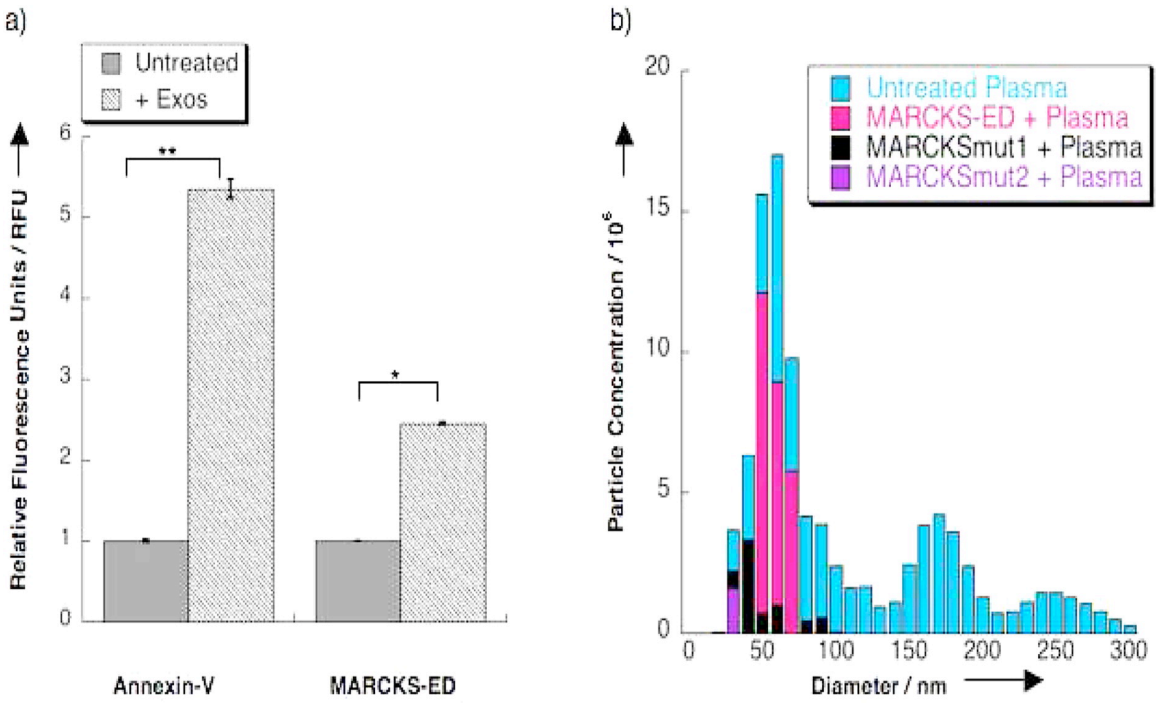

Figure 3.3 *Ex vivo* fluorescence assays. (a) Fluorescence enhancement of MARCKS-ED and Annexin-V after incubation with isolated rat extracellular vesicles. Fluorescence was normalized to the untreated NBD-MARCKS-ED peptide (0.5 μM) and Annexin-V (0.32 μM) samples. Fluorescence was normalized as 1.0 to the untreated protein or peptide samples in relative fluorescence units (RFU). **P value <0.01 compared to untreated samples. *P value <0.05 compared to untreated samples. (b) Nanoparticle tracking analysis results showing extracellular vesicles in plasma from stressed rats treated with fluorescently labeled MARCKS-ED at concentrations of 55 nM. The untreated plasma samples (blue) were detected using the scatter mode, and treated samples were monitored by tracking the fluorescence of Alexa Fluor 546 conjugated to the MARCKS-ED (pink), MARCKSmut1, and MARCKSmut2 (purple) peptides.

Figure 3.3a shows fluorescence enhancement with MARCKSED incubated with the isolated extracellular vesicles, demonstrating that MARCKS-ED can indeed bind to these biological particles. We further quantified the diameter size and particle count of the isolated extracellular vesicles detected by MARKCKS-ED. Nanoparticle tracking analysis (NTA) uses a laser source under either scatter or fluorescence detection mode to track small particles by Brownian motion, providing a robust method for analyzing vesicle size distribution (*13*). We first sought to detect the particles of all sizes in whole plasma samples from our stressed rat model under the scatter mode (Supplementary Video 1). Under the fluorescence mode with the emission filter set for the Alexa Fluor 546 label, the particles that bound to the MARCKS-ED (Supplementary Video 3), MARCKSmut1 (Supplementary Video 4), and MARCKSmut2 (Supplementary Video 5) peptides were observed. We found that MARCKS-ED selectively binds to exosomes (ϕ = 0.03−0.1 μm) in whole plasma (Figure 3.3b). MARCKSmut1 also showed some preferential binding to smaller vesicles but with much weaker fluorescence signal. The MARCKSmut2 peptide showed only negligible binding. Furthermore, tests with blank samples were performed to rule out possible artifacts caused by background fluorescence from the peptides, the vesicles (Supplementary Video 2) or the unconjugated dye (Supplementary Figure 11). Taken together, these data demonstrate that MARCKS-ED can selectively detect biologically relevant extracellular vesicles with highly curved, PS-enriched surfaces in a complex rat plasma solution.

Aiming to test our hypothesis that MARCKS-ED simultaneously detects shape and PS lipid composition, we further examined its ability to selectively bind to PS in live animals. We

carried out fluorescence staining assays in an established *C. elegans* model with PS-exposing cell membranes (*42*). PS is normally kept in the inner leaflet of plasma membranes in living cells and is exposed on the cell surface only under certain cellular events, i.e., when cells undergo apoptosis or lose the ability to maintain the PS asymmetry with a tat-1 gene mutation (*49*). Mutations of the tat-1 gene in *C. elegans*, which encodes for a phospholipid translocase that maintains PS plasma membrane asymmetry (*49*), resulted in PS externalization to the outer plasma membrane leaflet. Knockout of the ced-7 gene greatly reduced the macrophage clearance of apoptotic cell corpses with PS exposed on their cell surface (*49*). The NBD-labeled MARCKS-ED peptide was used to stain the dissected gonads of wild type (N2) animals, tat-1(tm3117) mutant animals, and engulfment-deficient ced-7 (n2094) mutant animals. As shown in Figure 4, MARCKS-ED can recognize PS exposed on the surface of all germ cells in the tat-1(tm3117) mutant and unengulfed apoptotic germ cell corpses in the ced-7(n2094) mutant without staining the wild type controls. By contrast, MARCKSmut1 did not appear to detect PS-exposing membranes in either tat-1 or ced-7 mutant animals, confirming that MARCKS-ED detects PS in a sequence-specific manner. Further, Annexin-V, a known PS-sensor, was also used to stain the gonads of tat-1 and ced-7 mutant animals. These staining results with MARCKS-ED were comparable to the staining results observed with Annexin-V (Supplementary Figure 12), indicating that MARCKS-ED may serve as a small peptide alternative to Annexin-V and detect PS exposed on the membrane surface in live animals.

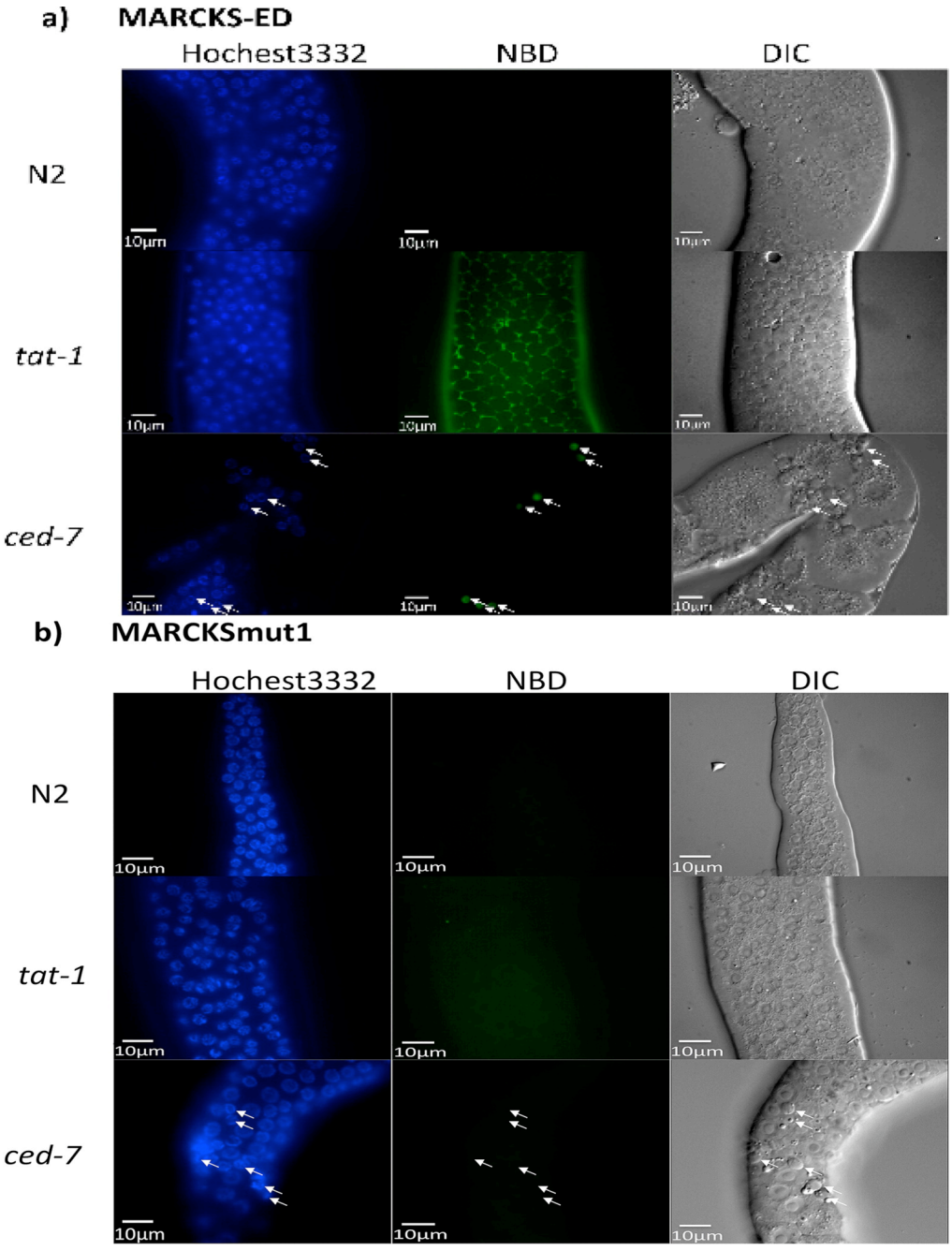

Figure 3.4 *In vivo C. elegans* fluorescence assay. The exposed gonads of a wild type N2 hermaphrodite animal (top row), a *tat-1(tm3117)* mutant animal (middle row), and a *ced-7(n2094)* mutant animal (bottom row) were stained with NDB-labeled (a) MARCKS-ED or (b)

MARCKSmut1. Images of Hoechst 33342 staining (cell nucleus), MARCKS peptide staining, and differential interference contrast (DIC) microscopy are shown. Arrowheads indicate apoptotic cell corpses. Scale bar = 10 μm.

3.5 Discussion.

In summary, the MARCKS-ED peptide was found to differentiate lipid vesicle sizes in both synthetic phospholipid models and extracellular vesicle generated in a rat animal model. Our data suggest that electrostatic interactions and aromatic Phe residues play a critical role in curvature sensing. MARCKS-ED may recognize PS-enriched, curved membranes by filling in the defects in asymmetrically stretched bilayers with its Phe residues, supported by the observation that its binding was greatly reduced with both MARCKSmut1 and MARCKSmut2 peptides. In vivo C. elegans studies confirmed specific detection of PS exposed on the membrane surface by the MARCKS-ED peptide. These results implies that MARCKSED could become a prototype for a new generation of peptide sensors that can simultaneously detect both PS and curvature and facilitate investigations of critical biological events, such as extracellular vesicles shedding and apoptosis.

CHAPTER 4

Probing Membrane Curvature Sensing Properties Using the MARCKS-ED Peptide

4.1 Abstract.

Curved membranes are a common and important attribute in cells. Protein and peptide curvature sensors are known to activate signaling pathways, initiate vesicle budding, trigger membrane fusion, and facilitate molecular transport across cell membranes. Nonetheless, there is more research required to understand how these proteins and peptides achieve preferential binding of different membrane curvatures. The current study is to elucidate specific factors required for curvature sensing. As a model system, we employed a recently identified peptide curvature sensor, MARCKS-ED, derived from the effector domain of the myristoylated alanine-rich C kinase substrate protein for these biophysical investigations. An atomistic molecular dynamics (MD) simulation suggested an important role; played by the insertion of the Phe residues within MARCKS-ED. To test these observations in computational simulation, we performed electron paramagnetic resonance (EPR) studies to determine the insertion depth of MARCKS-ED into differently curved membrane bilayers. Next, studies with varied lipid compositions revealed their influence on curvature sensing by MARCKS-ED, suggesting contributions from membrane fluidity, rigidity, as well as various lipid structures. Finally, we demonstrated that the curvature

sensing by MARCKS-ED is configuration dependent. In summary, our studies have shed further light to the understanding of how MARCKS-ED differentiates between membrane curvatures, which may be generally applicable to protein curvature sensing behavior.

4.2 Introduction.

Membrane curvature sensing is an important biological process. Nonetheless, the biophysical understanding of their molecular recognition is lacking. Many curvature sensing peptides and proteins share common structure and sequence characteristics (*27*). For example, the Bin/Amphiphysin/Rvs (BAR) domains, found in various membrane proteins such as Amphiphysin and Endophilin-A1 (*4, 45*), insert an amphipathic helix into the bilayer, acting as a wedge to create more space in the outer leaflet thereby causing membrane curvature (*50*). These proteins exude a more 'active' behavior, thus inducing membrane curvature. In another important study, Chapman and co-workers proposed that Synaptotagmin-1 exudes its 'passive' behavior to sense positive membrane curvature based on its membrane insertion mechanism (*3*). Synaptotagmin-1 uses its flexible loops stemming from two C2 domains to penetrate into the membrane bilayer of loosely packed lipids, another common feature of positively curved membranes (*3*). Lastly, electrostatic interactions have been suggested to be critical in stabilizing the interaction of protein domains on the membrane surface of highly curved regions (*1*). For instance, the positively-charged regions of the BAR domains have been shown to recognize highly curved membrane surfaces exposed with negatively charged acidic lipids (*1*).

Recently, our group has reported a novel 25 a.a. peptide, MARCKS-ED, derived from the effector domain of the myristoylated alanine-rich C kinase substrate (MARCKS) protein as a membrane curvature sensor (*22*). In fact, MARCKS-ED has been observed to localize in areas of positive curvature (*21*). Nonetheless, the molecular mechanism of its curvature sensing behavior remained elusive. In this current report, we employed a combination of various biophysical methods to investigate the basis of its curvature sensing behavior.

Based on previous biophysical electron paramagnetic resonance (EPR) results, we hypothesized that insertion of aromatic residue side chains significantly contribute to its curvature sensing, which is in agreement with previous reports that the Phe residues in the effector domain of MARCKS-ED were buried (*18*). Next, fluorescence enhancement experiments were performed using both L- and D-MARCKS-ED peptides to study whether the peptide recognizes curvature in a configuration-specific manner. To further expound on these fluorescence enhancement findings, we quantified the binding affinities of MARCKS-ED to differently sized lipid vesicles. Next, electron paramagnetic resonance (EPR) was used to determine the insertion depth of the Phe residues into lipid vesicles presenting different curvatures.

Membrane composition also gives rise to membrane curvature primarily dictated by the shape and charge of their lipid components (*51, 52*). Lipids have long been known to have significant functions in membrane shape, mobility, and stiffness (*53*). Importantly, lipid packing induces defects, which was suggested to play a role in curvature sensing (*7*). Therefore, we next studied the impacts of various lipid components in biologically relevant membranes on the

curvature sensing ability of MARCKS-ED, revealing the importance of peptide-lipid interactions in the recognition of membrane curvature.

Taken together, we herein report that Phe insertion in conjunction with specific peptide-lipid interactions could contribute to the membrane curvature sensing by MARCKS-ED. These results could help successfully design novel membrane curvature probes for studying biological processes.

4.3 Experimental Methods.

Solid Phase Peptide Synthesis. All peptides were synthesized using a CEM Liberty microwave-assisted solid phase peptide synthesizer using standard Fmoc chemistry. The natural L-form of the MARCKS-ED peptide, the mirror image D-form of the MARCKS-ED peptide and the mutant FA-MARCKS-ED peptide, generated by mutating Phe to Ala, were conjugated to a 6-(N-(7-Nitrobenz-2-oxa-1,3-diazol-4-yl)amino)hexanoic acid (NBD) fluorophore to the N-terminus via an aminohexanoic acid linker. For electron paramagnetic resonance (EPR) studies, the 11th position, Lys residue, from the MARCKS-ED peptide was mutated to a Cys residue to conjugate the methanethiosulfonate (MTSL) label, generating the peptide MTSL-K11C. Following NBD or MTSL conjugation, the resin beads were then washed, dried and cleaved from the peptide using a water/trifluoroacetic acid (TFA)/ triisopropylsilane (TIPS) cocktail for 1 hour under inert conditions. Chilled diethly ether was used to precipitate the peptides. Reverse phase high performance liquid chromatography was performed to purify each peptide using a semi-prep C8 column.

Lipid Vesicle Preparation. To generate homogeneous lipid vesicle solutions, a previously reported protocol was followed (*28, 29, 34*). The following lipids were purchased from Avanti Polar Lipids: 1-palmitoyl-2-oleoyl-*sn*-glycero-3-phosphoethanolamine (POPE), 1-palmitoyl-2-oleoyl-*sn*-glycero-3-phospho-L-serine (POPS), L-phosphatidylcholine (POPC), sphingomyelin and cholesterol. The lipid content was based on reported approximations of the lipid composition exposed on the outer leaflet of exosomes (*54*). After mixing each lipid component, the organic solvent was removed using a slow flow of nitrogen until a thin, white film was observed on the bottom of the glass vial. Each glass vial was placed in the dessicator *in vacuo* for at least 30 minutes. Phosphate buffer (pH = 7.40) was added to each glass vial containing the dry film and incubated overnight to hydrate at 4°C. A summary of the lipid compositions of the different vesicle systems studied is found in Table 4.1.

The lipid vesicle solutions were extruded by an Avestin FL-50 pressurized extruder using polycarbonate membranes purchased by Avanti Polar Lipids. An established protocol was carried out (*34*). The polycarbonate membrane filters used were of sizes 30, 100 and 400 nm. For each lipid vesicle size, the lipid vesicle solutions were extruded through the membrane filters at least 3 times to generate homogeneity. To characterize the actual vesicle diameter for each lipid vesicle solution, we used the nanoparticle tracking analysis (NTA) to produce a distribution curve displaying the vesicle size present in each solution. The LM10-HS instrument was used with a 638 nm laser at scatter mode and a 650 nm laser at fluorescence mode. Figure 4.1 shows the stability of all lipid compositions for each vesicle size produced.

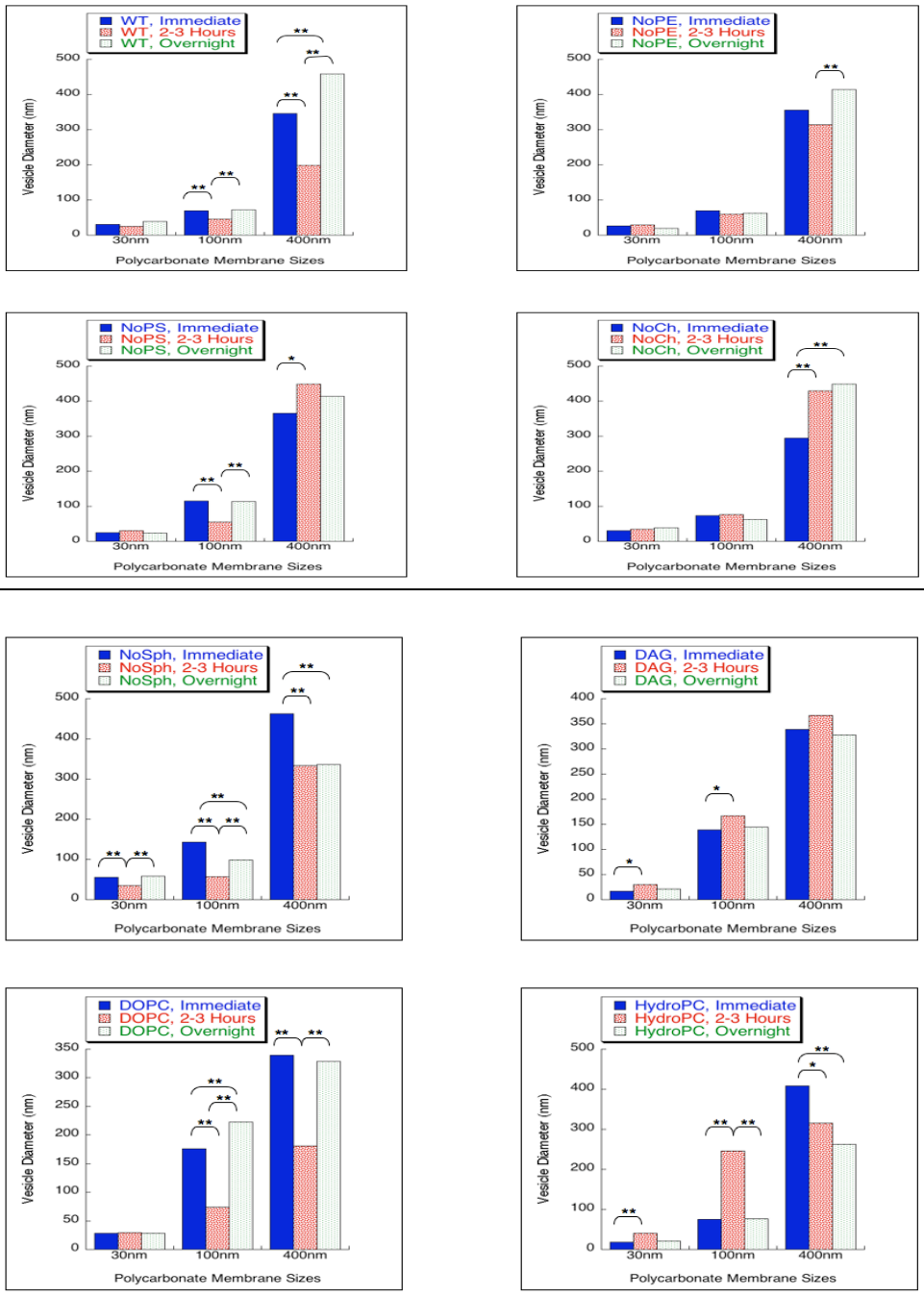

Figure 4.1 The stability of vesicles as indicated by the vesicle diameters measured at different

time points. Lipid compositions are described in Table 4.1. *P value < 0.05. **P value < 0.01.

Fluorescence Enhancement Assay. The Fluorolog-3 fluorometer by Horiba Jobin Yvon was used to observe emission spectra for NBD-labeled MARCKS-ED peptides. Excitation and emission wavelengths were set at λ_{ex} = 480 nm and λ_{em} = 545 nm for the NBD fluorophore. Proper controls were performed to ensure that the observed fluorescence intensity was solely based on the peptide and not on the fluorophore (*22*). The MARCKS-ED peptides (500 nM) were incubated with each lipid vesicle solution (500 μM) in PBS (pH = 7.40) prior to the experiment. The fluorescence emission spectrum was set from 500-650 nm.

Fluorescence Anisotropy Assay. Fluorescence anisotropy was performed using the Horiba Jobin Yvon Fluorolog-3 fluorometer. Each concentrated lipid vesicle size was titrated into the MARCKS-ED peptide solution until the binding curve reached saturation. The excitation and emission wavelengths were set to λ_{ex} = 480 nm and λ_{em} = 545 nm for the NBD fluorophore. As previously reported (*43*), the following equation was used to measure the apparent binding affinity, K_D:

$$Fb = Kp[L]/(1 + Kp[L]) \quad (1)$$

Equation 4.1 Solving for the apparent binding affinity, K_D. This equation describes Fb as the fraction of peptide bound to the lipid vesicles, Kp describes the molar partition coefficient and

[L] describes the lipid concentration. This equation was fitted to each anisotropy graph where the Kp is expressed as the inverse of the apparent dissociation constant, K_D.

Electron Paramagnetic Resonance (EPR). EPR was performed to study the interactions of the mutated MARCKS-ED peptide, MTSL-K11C, with different-sized vesicles. Methanethiosulfonate (MTSL) provides the unpaired electron required for an EPR response. The EPR spectra and data were gathered using a Bruker Elexsys E500 spectrometer and a loop gap resonator. To determine the depth parameter values of the MTSL-K11C peptide within the membrane bilayer, EPR power saturation experiments were performed by incrementally increasing the power of the instrument while recording the changes of the amplitude of the central resonance peak until saturation of the electron spin is reached. Equations from Scheme 4.1 describe how the depth parameter was measured. The power at which the system was at half saturation, $P_{1/2}$, was calculated based on Eq. S1. The $P_{1/2}$ values describe the frequency of collisions between the nitroxide label, MTSL, and the O_2 or NiEDDA probes. The $P_{1/2}$ value is then used to solve for the solvent accessibility, π, for both paramagnetic probes, O_2 and NiEDDA using Eq. S2, respectively. A higher π value points to more collision frequencies between the paramagnetic probe with the nitroxide-labeled K11C peptide, MTSL-K11C. The solvent accessibility values are required to calculate the depth parameter values (Φ).

Eq. 3: $A = c^{*}P^{1/2}[1 + (2^{1/\varepsilon} - 1)\, P/P_{1/2}]^{-\varepsilon}$

Eq. 4: $\pi(x) = [(P_{1/2}(x)/\Delta H_{pp}(x)) - (P_{1/2}(N_2)/\Delta H_{pp}(N_2))] / [P_{1/2}(DPPH)/\Delta H(DPPH)]$

x = Under O_2 or NiEDDA, N_2

Eq. 5: $\phi = \ln[\pi(O_2) / \pi(NiEDDA)]$

Scheme 4.1 A list of equations to determine the depth parameters (Φ) using EPR power saturation. Equation variables are described as the following: C represents the scaling factor, ε represents the homogeneous factor (1.5=homogenous and 0.5=heterogenous), $P_{1/2}$ represents the power at half saturation, ΔH_{pp} represents the average line width of the central resonance peak. DPPH is an EPR standard, defined as di(phenyl)-(2,4,6-trinitrophenyl)iminoazanium.

4.4 Results.

MARCKS-ED Senses Curvature in a Configuration-Specific Manner. To further explore the molecular recognition of MARCKS-ED to differently curved membranes, we next carried out fluorescence enhancement assays with MARCKS-ED along with its mirror-image peptide D-MARCKS-ED, composed of unnatural, D-amino acids, which was synthesized and performed by Ryo Tamura. Fluorescence enhancement describes a change in fluorescence intensity brought about by the environmental change surrounding the fluorophore conjugated to the N-terminus of each peptide from a polar, aqueous solvent to a hydrophobic bilayer. An increase in fluorescence intensity indicates peptide-vesicle binding. Vesicles with various percentages of the cationic lipid, phosphatidylserine (PS), were used in these experiments as previous studies showed that

PS contributes to most of the binding affinity of MARCKS-ED (*22*). It is highly interesting to observe that, in contrast to the natural L-MARCKS-ED, D-MARCKS-ED does not distinguish between different membrane curvatures at any given PS concentration (Figure 4.2). As observed in Figure 4.2, the L-MARCKS-ED appears to bind weakly to 400 nm; whereas, the D-MARCKS-ED binds strongly to all vesicle sizes. Curvature sensing behavior is observed as weaker binding to 400 nm vesicles relative to smaller vesicles for the L-MARCKS-ED peptide. This observation could suggest that the D-MARCKS-ED peptide may be adopting secondary structures in contrast to the L-MARCKS-ED peptide. Contrasting fluorescence results between these two peptides, different based only on configuration, would propose that peptide configuration may influence how MARCKS-ED interacts with different vesicles. Specifically, as L-MARCKS-ED binds to larger vesicles, electrostatic interactions may be more hindered with larger vesicles presumably created by larger defects exposed on the membrane surface. The D-MARCKS-ED may adopt another secondary structure, in contrast to the unstructured conformation observed by the L-MARCKS-ED, so as to overcome any potential interference with phosphatidylserine interaction.

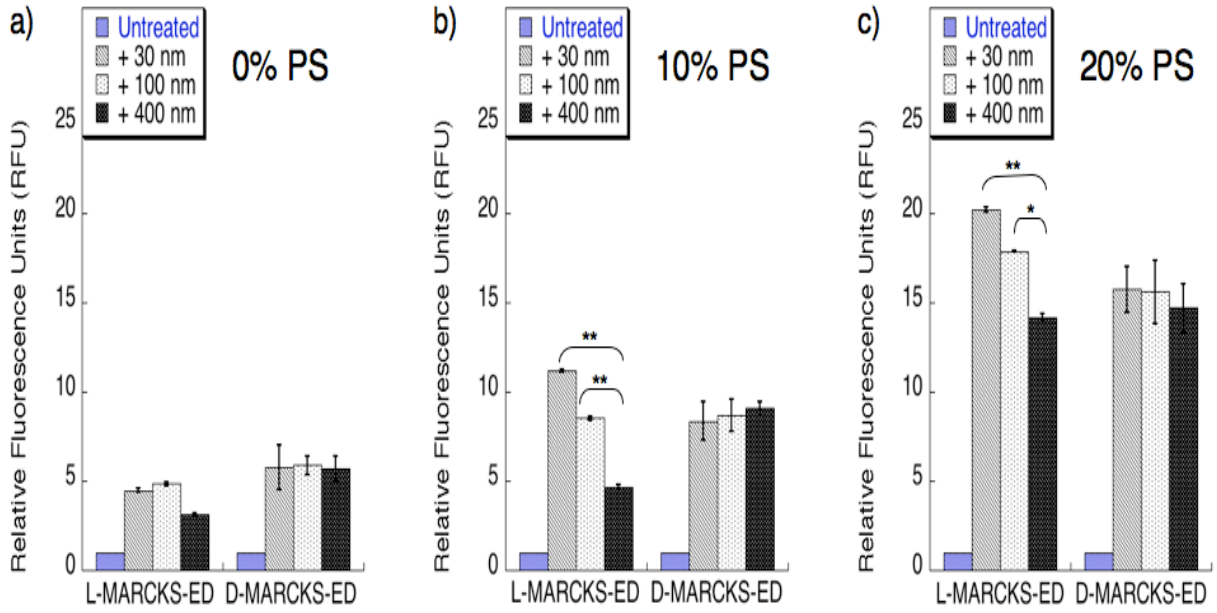

Figure 4.2 Fluorescence enhancement results comparing L-MARCKS-ED and D-MARCKS-ED peptides. Fluorescence enhancement assay displaying the maximum fluorescence intensity from the NBD label attached to the N-terminus of both the natural L- and un-natural D-MARCKS-ED peptides. [Peptide] = 500 nM. [Lipid vesicle] = 500 μM. Fluorescence (in relative fluorescence units, RFU) was normalized to the untreated MARCKS-ED peptides. *P value < 0.01 compared to 400 nm polycarbonate membrane pores. **P value < 0.05 compared to 400 nm polycarbonate membrane pores.

Characterizing the Contribution of Binding Affinity in Curvature Sensing. Fluorescence enhancement solely indicates the average change in the environment of the fluorophore conjugated to MARCKS-ED, from a polar to a more hydrophobic one. This average change could be dissected into two different factors: different insertion depth and binding affinities. To

measure the respective contributions of these two factors, we first carried out a fluorescence anisotropy assay to determine the differences in binding affinity. Lipid vesicles with different diameters (small vesicles present surfaces with more curvature) were titrated to the NBD-labeled MARCKS-ED, which results in an increase in polarization upon peptide-vesicle association. The dissociation constant (K_D) values of MARCKS-ED with lipid vesicles of 30-, 100- and 400-nm diameters were determined to be 14 ± 1 μM (compared to 400 nm, $P < 0.01$), 17 ± 2 μM (compared to 400 nm, $P < 0.01$), and 33 ± 2 μM, respectively. This preferential binding is comparable with literature reports that Synaptotagmin-1 (Syt-1) shows a 1.9-fold increase in binding affinity between small (d=105 nm) and large (d=252 nm) vesicles (*3*).

Characterizing the Contribution of Different Insertion Depths in Curvature Sensing. The MD simulations suggested the importance of the Phe residues in MARCKS-ED binding. To explore the second contributing factor of different insertion depths, which may influence curvature sensing by MARCKS-ED, electron paramagnetic resonance (EPR) spectroscopy was performed. Previous studies with one-fixed sized vesicles (d= 100 nm) showed that MARCKS-ED penetrated into membrane bilayers (*18*). Herein, the interaction of MARCKS-ED with vesicles of different sizes was explored. Figure 4.3 shows spectra for the methanethiosulfonate (MTSL, a commonly used paramagnetic probe)-labeled MARCKS-ED, MTSL-K11C, in the presence (red) and absence of lipid vesicles (blue). Consistent with a previous report (*18*), EPR spectra with lipid vesicles all showed significant peak broadening, indicative of the reduced MTSL-K11C tumbling rate caused by its membrane association.

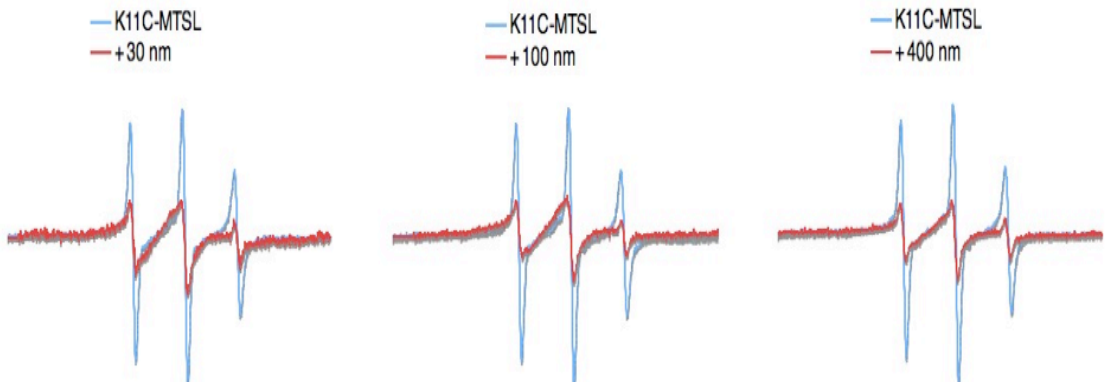

Figure 4.3 EPR line spectra. These plots showing the methanethiosulfonate-labeled MARCKS-ED bound to different sized synthetic lipid vesicles with the wild type lipid model (Table 4.1). Binding has reached saturation at the tested peptide-lipid ratio (*18*).

To measure the depth of MARCKS-ED insertion into different membrane curvatures, power saturation experiments were performed for each lipid vesicle size. Figure 4.4 shows the power saturation curves for each vesicle size in the absence (red curve) of and presence of the paramagnetic probes O_2 and NiEDDA (blue and green curves, respectively). Measurements of the probe-free and the NiEDDA-containing vesicles were performed under N_2. Figure 4.4 describes the measured amplitude values of the central resonance peak (as shown in Figure 4.3) plotted against the square root of the microwave power for each vesicle size. The complex ion NiEDDA and O_2 form concentration gradients across the plasma membrane. Specifically, this suggests that O_2 is more concentrated within the membrane bilayer and NiEDDA is more concentrated in the aqueous solution. Two samples are prepared for each lipid vesicle size

solution: in the (1) absence and (2) presence of the NiEDDA complex. If our nitroxide-labeled peptide is interacting more so within the membrane bilayer than in the aqueous solution, more nitroxide collision frequencies will take place between O_2 and our K11C-MTSL peptide relative to the complex ion NiEDDA. These interactions will create relaxation of the nitroxide signal since spin-spin exchange will occur between O_2 and our K11C-MTSL peptide, resulting in more power being required to reach saturation. Saturation is reached when the all unpaired electrons have been excited to the highest energy level; thus, the amplitude of the central resonance peak reaches its maximum. As observed in Figure 4.4, three plots are defined for each vesicle size: without NiEDDA under (1) O_2, (2) N_2 and (3) with NiEDDA (under N_2). Power saturation was performed with solutions that included NiEDDA in the presence of N_2 to avoid any potential O_2 signal that could interfere with interactions solely created by the NiEDDA complex. It was critical to perform power saturation experiments in the presence of N_2 for normalization purposes, since in this case, there is an absence of both paramagnetic probes O_2 and NiEDDA. The N_2 experiment is to compensate for other ways the nitroxide label can be relaxed. The N_2 measurements are subtracted by those recorded from both the NiEDDA and O_2 as described in Scheme 4.1. Using the equations summarized in Scheme 4.1, the depth parameter (Φ) can be calculated.

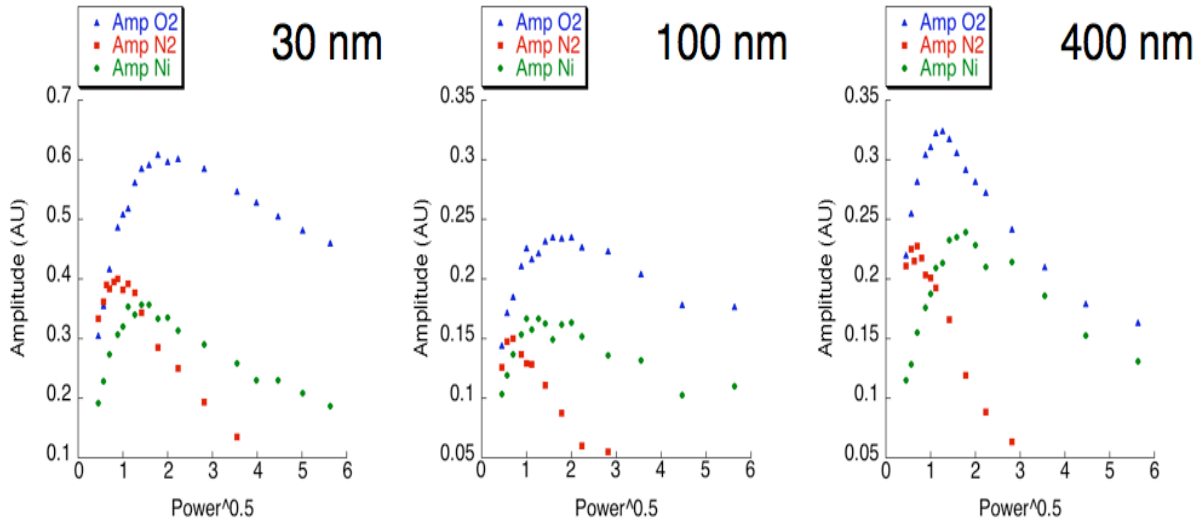

Figure 4.4 EPR power saturation plots. The methanethiosulfonate-labeled MARCKS-ED, MTSL-K11C, with synthetic lipid vesicles of 30 nm, 100 nm and 400 nm diameters. Power saturation was performed under O_2, and under N_2 with and without the paramagnetic NiEDDA probe.

The depth parameter Φ values were then calibrated using five commercially available, spin-labeled nitroxide phosphatidylcholine (PC) lipids. The head group labeled PC was given a value of -5 Å based on a previous report (*18*). These lipids are labeled with doxyl nitroxides at positions C5, C7, C10 and C12 on the acyl chain as well as on the head group, respectively (*18*). The calibration plots display a linear correlation between the distance of the probe on the lipid chain relative to the membrane bilayer and their depth parameters (Figure 4.5), confirming that Φ values (as shown in Figure 4.6) is a valid measurement of insertion depth. It is important to mention that these experiments were performed only once, thus, error bars could not be included.

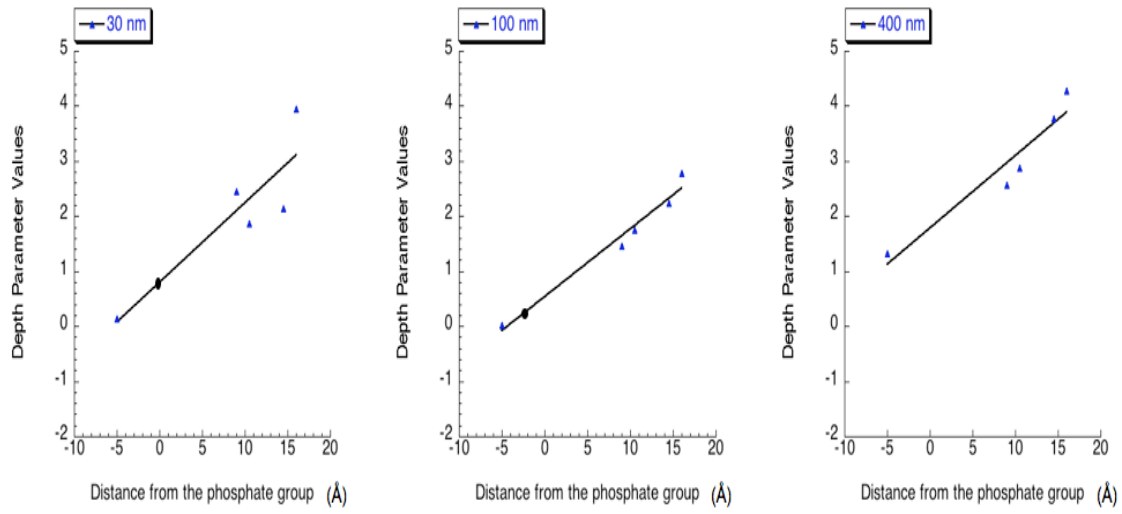

Figure 4.5 EPR calibration curves. The following calibration curves were performed using spin-labeled lipids (*18*) purchased from Avanti for each vesicle size of 30 nm, 100 nm and 400 nm. The lipid composition used the wild type lipid model (Table 4.1). The *n*-doxyl PC with spin label at C 5, 7, 10, 12, along at the head group.

The distance of the MTSL label in MTSL-K11C from the phosphate group was calculated as shown in Figure 4.6b (a more negative value indicates a position further from the bilayer center). Despite consistently observing larger depth insertion values (more positive) for smaller vesicle sizes relative to larger vesicle sizes, we cannot confidently conclude that MARCKS-ED inserts more deeply into highly curved membrane bilayers based on the large standard error observed in Figure 4.6. This large standard error could be based on a few explanations.

The standard deviation measured was based on the depth insertion values determined from different power saturation experiments for the lipid vesicle solutions performed on different days. It is probable that a low signal could influence the variability of the depth insertion values since the resolution of the amplitude recorded for each power value is based on the signal of the solution. A low signal would present an unresolved EPR spectrum with jagged lines observed for the amplitude peaks, potentially allowing an error in observing the true amplitude maximum. Furthermore, the signal is based on the nitroxide spin label concentration. It is probable that the concentration of nitroxide-labeled peptide could be inaccurate based on the way the concentration is calculated. Conventionally, the nitroxide-labeled MARCKS-ED peptide is measured through Phe absorbance by UV-vis spectroscopy; however, this takes into account of all the peptide in solution instead of only nitroxide-labeled MARCKS-ED peptide. The nitroxide spin label is unable to absorb light so this is the standard way of measuring the concentration. An increase in nitroxide label for maximum conjugation as well as optimal purification methods could resolve this potential issue.

Furthermore, the vesicle stability over time may also have an effect on different depth insertion values observed. The vesicle diameter is measured for each size prior to experiments; however, subtle changes in vesicle size determination from each extrusion process performed on different days may influence the binding interaction of the K11C-MTSL peptide with these vesicles. Specifically, one week may record a 40 nm vesicle size for the 30 nm polycarbonate pore; whereas, the following week may record a 25 nm vesicle size for the same pore size.

Lastly, binding saturation could also be a variable affecting the EPR spectrum observed by the K11C-MTSL peptide with different vesicles. Although vesicle and peptide concentrations used for these experiments were rationally chosen to match what has previously been found to show binding saturation between the MARCKS-ED peptide and lipid vesicles, a series of concentrations could be performed to compare the differences in EPR spectra to confirm binding saturation prior to power saturation experiments and depth insertion determinations.

a)

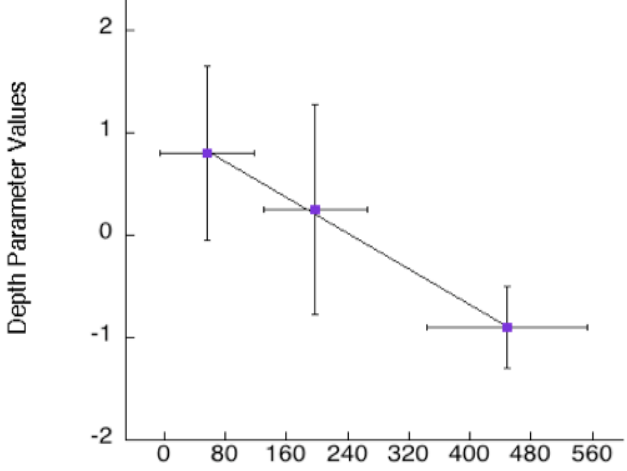

b)

Vesicles (nm)	Depth Parameters (ϕ)	Distance from phosphate group (more positive: closer to bilayer center) (Å)
30	0.8053 ± 0.85	± 0
100	0.2509 ± 1.03	~ -2.5
400	-0.90048 ± 0.404	< -5.0

Figure 4.6 EPR plot showing the correlation between the depth parameters and different vesicle sizes. a) These results demonstrate that MARCKS-ED inserts more deeply in the membrane

bilayer with more curvatures. b) The table describes a list of each synthetic lipid vesicle size describing its depth parameters (Φ) and distance from the membrane bilayer (Å).

Does Lipid Composition Influence Curvature Sensing? To explore the role of lipids in MARCKS-ED curvature sensing behavior, we measured its binding affinity towards vesicles with different lipid composition and sizes (Table 4.1). A mutant MARCKS-ED, referred to as FA-MARCKS-ED, in which the Phe residues were replaced with Ala was used as a control. Figure 4.7 shows bar plots where the dissociation constants (K_D) measured for each lipid model were normalized based on the dissociation constant between the wild type MARCKS-ED peptide bound to the 30 nm lipid vesicle size of the wild type lipid model. In vesicles consisting of the wild type membrane model, MARCKS-ED binds to smaller vesicles of more curvature with significantly higher affinity. We observed similar results in the vesicles lacking sphingomyelin, suggesting that sphingomyelin has no apparent contribution in MARCKS-ED curvature sensing behavior. We previously showed that in the absence of phosphatidylserine (PS), the preferential binding of MARCKS-ED was compromised (*22*). Herein, we find that phosphatidylethanolamine (PE), or cholesterol (Figure 4.7a, NoPE and NoCh, respectively) are also required for MARCKS-ED's curvature sensing. Across all these lipid systems, FA-MARCKS-ED does not show any size discrimination (Figure 4.7b), confirming the critical role of the Phe residues.

Lipid Models	Lipid Composition
WT (Wild type)	28% POPC: 27% POPE: 17% POPS: 14% Chol: 14%Sph
NoPE	55% POPC: **0% POPE**: 17% POPS: 14% Chol: 14%Sph
NoPS	45% POPC: 27% POPE: **0% POPS**: 14% Chol: 14%Sph
NoSp	42% POPC: 27% POPE: 17% POPS: 14% Chol: **0%Sph**
NoCh	42% POPC: 27% POPE: 17% POPS: **0% Chol**: 14%Sph
DAG	28% POPC: **27% DAG:** 17% POPS: 14% Chol: 14%Sph
Hydro-PC	28% POPC: 27% POPE: 17% POPS: **14% Hydro-PC**: 14%Sph
DOPC	28% POPC: 27% POPE: 17% POPS: **14% DOPC**: 14%Sph

Table 4.1 A list of different synthetic lipid vesicles prepared for biophysical assay. Wild type (WT) models represent a composition closely resemble exosome cell membranes (*54*).

Characterizing PE's Role in MARCKS-ED's Curvature Sensing. To further understand why both PE and cholesterol are critical to MARCKS-ED's curvature sensing behavior, we chose to replace each of these lipids with another lipid component having similar structural characteristics to determine whether any rescue of curvature sensing behavior could be observed. First, we replaced PE with diacyl glycerol (DAG), a lipid sharing a common conical shape with PE (*53*). The removal of PE from wild type vesicles eliminated vesicle size distinction (Figure 4.7a, NoPE). Upon replacement of the PE with DAG (Figure 4.7a, DAG), no significant rescue of curvature sensing was observed. The FA-MARCKS-ED mutant peptide measured stronger binding affinities for the DAG mutant model relative to all the other lipid models. Although

smaller K_D values were observed, there is only a slight difference between the 30- and 400-nm vesicle solutions and thus did not exceed the 1.9 fold binding affinity difference to be considered curvature sensing behavior.

Characterizing Cholesterol's Role in MARCKS-ED's Curvature Sensing Cholesterol is known to modulate membrane fluidity by the ability to either increase or decrease bilayer rigidity – the former in fluid bilayers and the latter, in gel-phase bilayers (*55, 56*). To explore the role that cholesterol plays in the context of highly curved vesicles and how it relates to MARCKS-ED's curvature sensing behavior, we replaced cholesterol with hydrogenated-phosphatidylcholine (Hydro-PC) to probe the fluidity-decreasing role and dioleoyl-glycero-phosphocholine (DOPC) to examine the fluidity-enhancing role of membrane bilayers. Hydro-PC contains fully saturated lipid tails and thus, increases lipid packing and decreases membrane fluidity (*57*). On the other hand, DOPC can decrease lipid packing and increase membrane fluidity due to its two unsaturated lipid tails (*57*). From Figure 4.10a (Hydro-PC), there was also a change in binding affinity between 30- and 400 nm lipid vesicles with the replacement of cholesterol by Hydro-PC. In comparison with the replacement of cholesterol by DOPC (Figure 4.7a, DOPC), less significant binding affinity differences among different vesicle sizes were revealed. In comparison to the wild type MARCKS-ED peptide, the FA-MARCKS mutant did not show vesicle size discrimination similarly as the wild type MARCKS-ED peptide where stronger binding was shown for smaller vesicles (d=30 nm) versus larger vesicles (d=400 nm). In contrast, we did however observe stronger binding to the larger vesicles (d=400 nm) relative to the smaller vesicles (d= 30 and 100 nm). This unexpected observation could be explained by a potential difference in lipid concentration within the 400 nm vesicle solution. To produce large lipid vesicle

solutions, less nitrogen is required for extrusion and perhaps, a larger molar amount of lipids could be present in solution, affecting binding interaction and saturation with the MARCKS-ED peptide.

Furthermore, if the lipid concentration is indeed the same as expected, the differing binding affinities could be based on the lack of Phe insertion, which could be interfering with electrostatic interactions for larger vesicles. Without Phe, Ala is spatially smaller and not observed to insert into the membrane by previous studies. This Ala residue could allow the MARCKS-ED peptide to interact differently by binding to areas of the larger vesicles with more localized PS and less surface defects since Phe insertion would not have to be accommodated for membrane binding interaction. It is important to mention that although FA-MARCKS-ED bound tighter to larger vesicles relative to smaller ones, the dissociation constant for the larger vesicle (d=400 nm) was still higher relative to those measured by the wild type MARCKS-ED peptide. This observation supports the importance of the Phe residues and how these residues may be contributing to the overall binding energy.

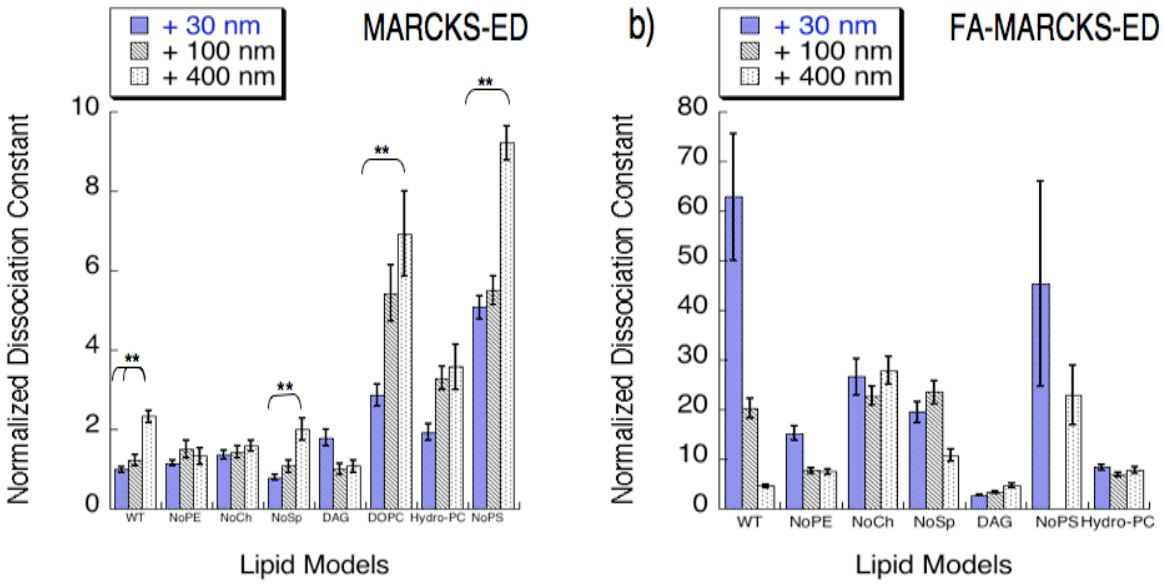

Figure 4.7 Membrane curvature sensing by a) MARCKS-ED and b) FA-MARCKS-ED in vesicles with different lipid composition. K_D values were determined by fluorescence anisotropy assays for each lipid vesicle size and composition (Table 4.2). For direct comparison, all K_D values were normalized to that of the wild type 30 nm vesicle size by the MARCKS-ED peptide. Asterisks (**) indicate curvature sensing behavior. Many of these lipid fluorescence studies were performed in collaboration with Arianna Espinoza. *P value < 0.01 compared to 400 nm polycarbonate membrane pores. **P value < 0.05 compared to 400 nm polycarbonate membrane pores.

MARCKS-ED:

Polycarbonate Membrane Pores (nm)	WT (Wild type) K_D (μM)	NoPE K_D (μM)	NoPS K_D (μM)	NoCh K_D (μM)	NoSp K_D (μM)	DAG K_D (μM)	DOPC K_D (μM)	Hydro-PC K_D (μM)
30	14 ± 1	16 ± 1	71 ± 4	19 ± 1.5	11 ± 1	25 ± 3	40 ± 4	8 ± 1
100	17 ± 2	21 ± 3	77 ± 5	20 ± 2	15 ± 2	14 ± 2	76 ± 10	27 ± 4
400	32.5 ± 2	18.5 ± 3	129 ± 6	22.2 ± 2	28 ± 4	15 ± 2	97 ± 15	50 ± 9

FA-MARCKS-ED:

Polycarbonate Membrane Pores (nm)	WT (Wild type) K_D (μM)	NoPE K_D (μM)	NoPS K_D (μM)	NoCh K_D (μM)	NoSp K_D (μM)	DAG K_D (μM)	DOPC K_D (μM)	Hydro-PC K_D (μM)
30	880 ± 179	213 ± 21	2850 ± 1300	372 ± 51	273 ± 30	39 ± 2	112 ± 10	117 ± 7
100	284 ± 17	108 ± 7	N/A	319 ± 27	329 ± 33	46 ± 3	78 ± 7	96 ± 7
400	64 ± 5	105 ± 7	1439 ± 375	390 ± 38	151 ± 16	65 ± 6	172 ± 20	109 ± 8

Table 4.2 A list of dissociation constants (K_D). These dissociation constants measured for the various lipid vesicle compositions and sizes for both MARCKS-ED and FA-MARCKS-ED.

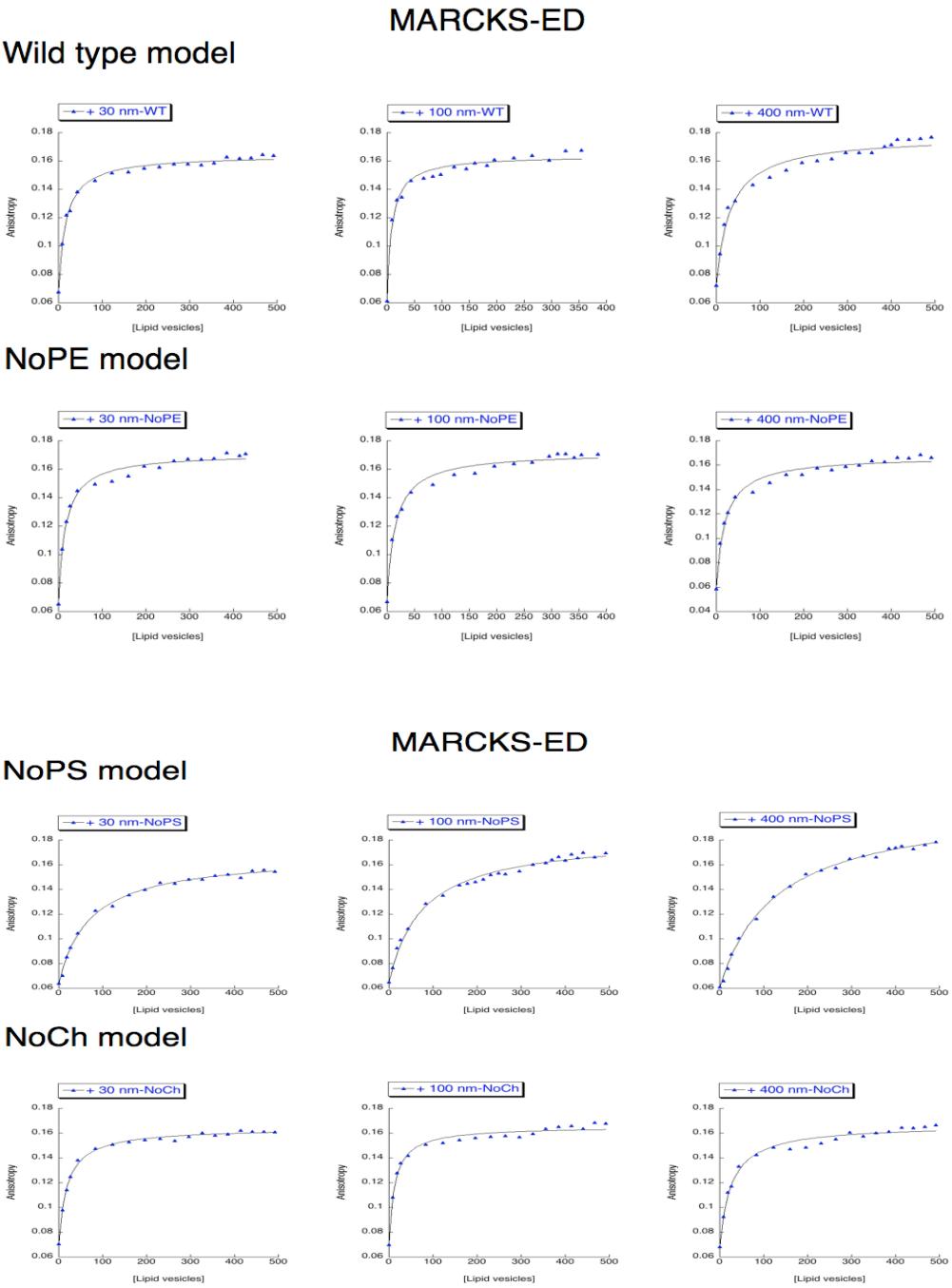

Figure 4.8 Anisotropy plots of MARCKS-ED with different lipid models described in Table 4.1 and normalized for Figure 4.7. Lipid models include: wild type, NoPE, NoPS and NoCh.

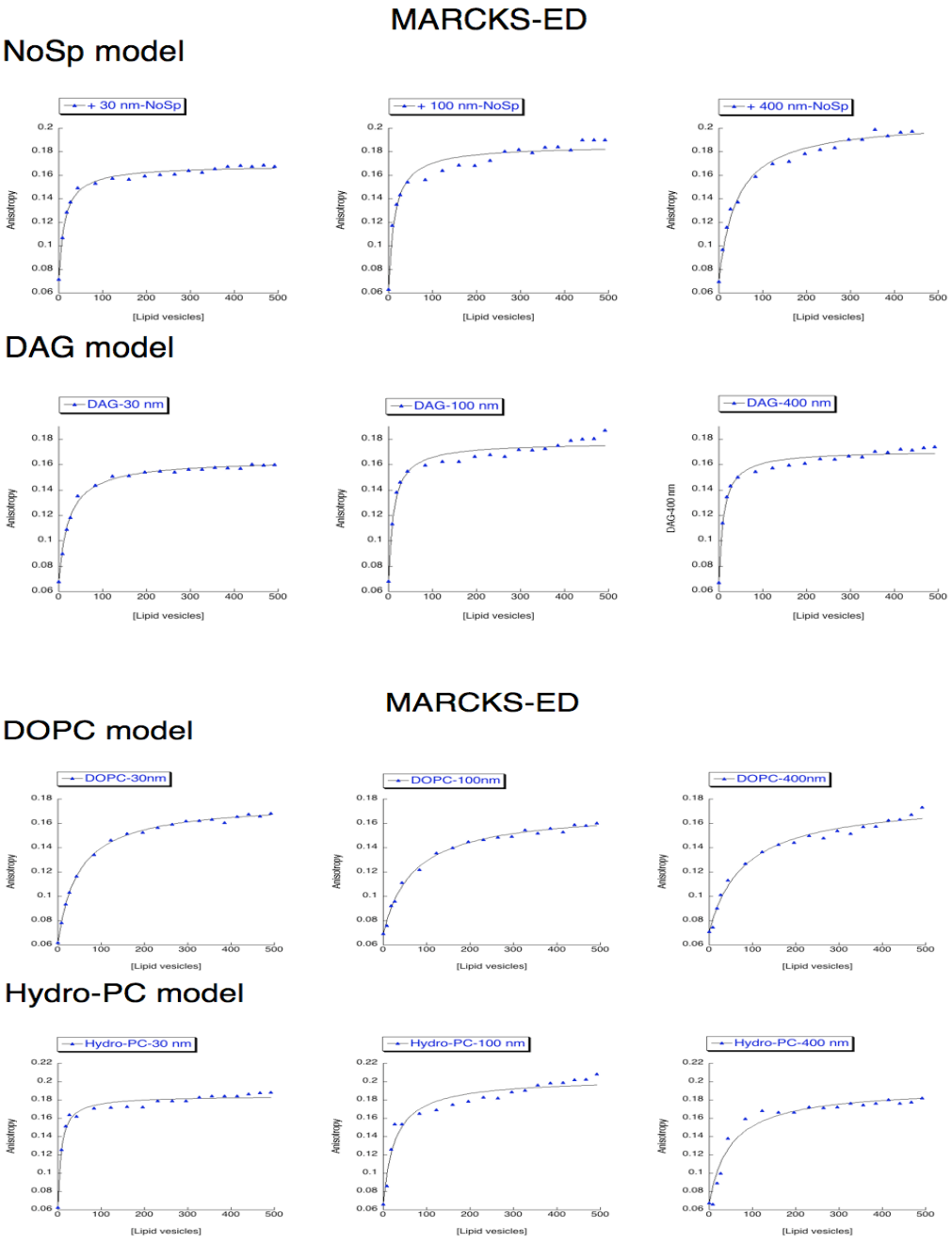

Figure 4.9 Anisotropy plots of MARCKS-ED with different lipid models described in Table 4.1 and normalized for Figure 4.7. Lipid models include: NoSp, DAG, DOPC and Hydro-PC.

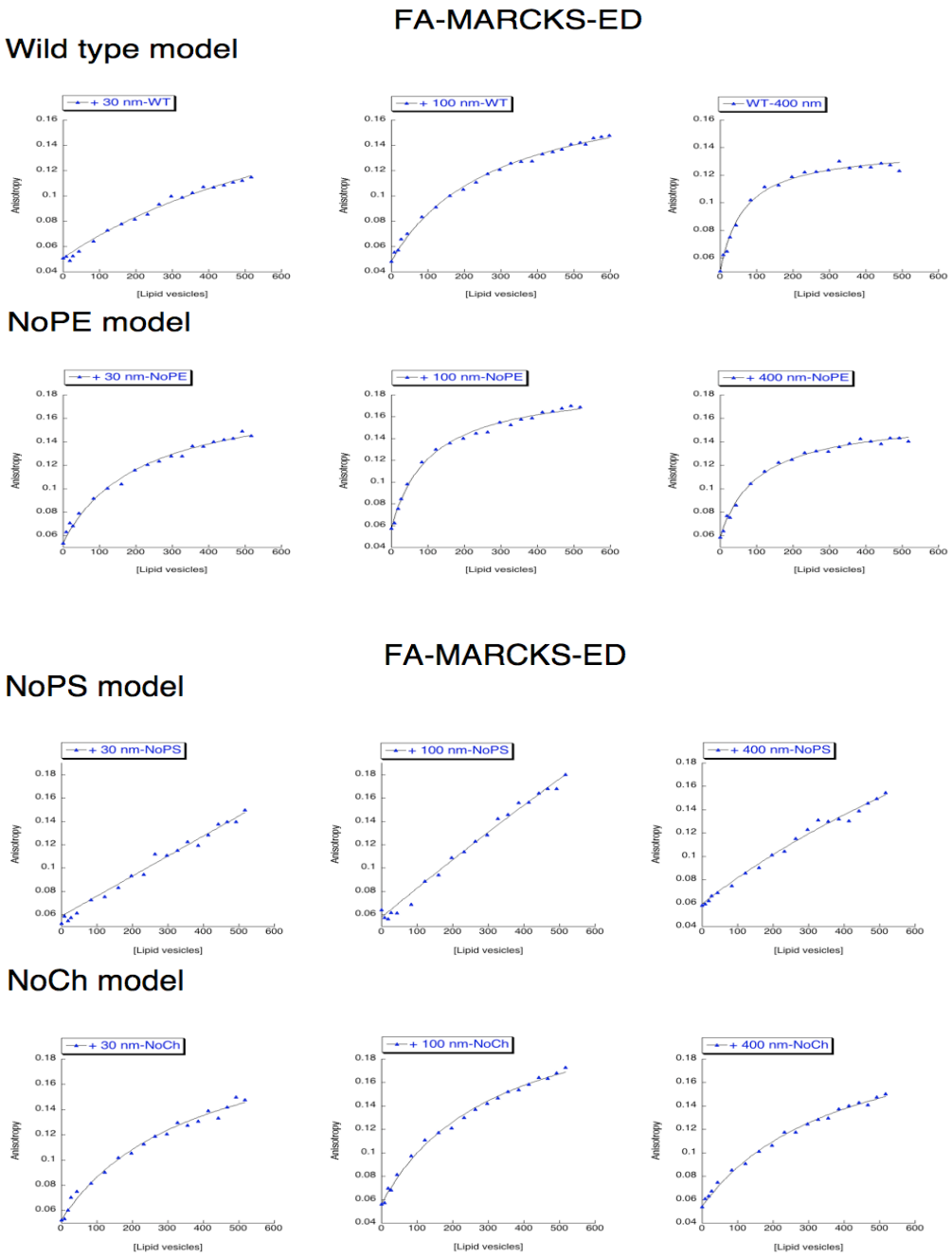

Figure 4.10 Anisotropy plots of FA-MARCKS-ED with different lipid models described in Table 4.1 and normalized for Figure 4.7. Lipid models include: wild type, NoPE, NoPS and NoCh.

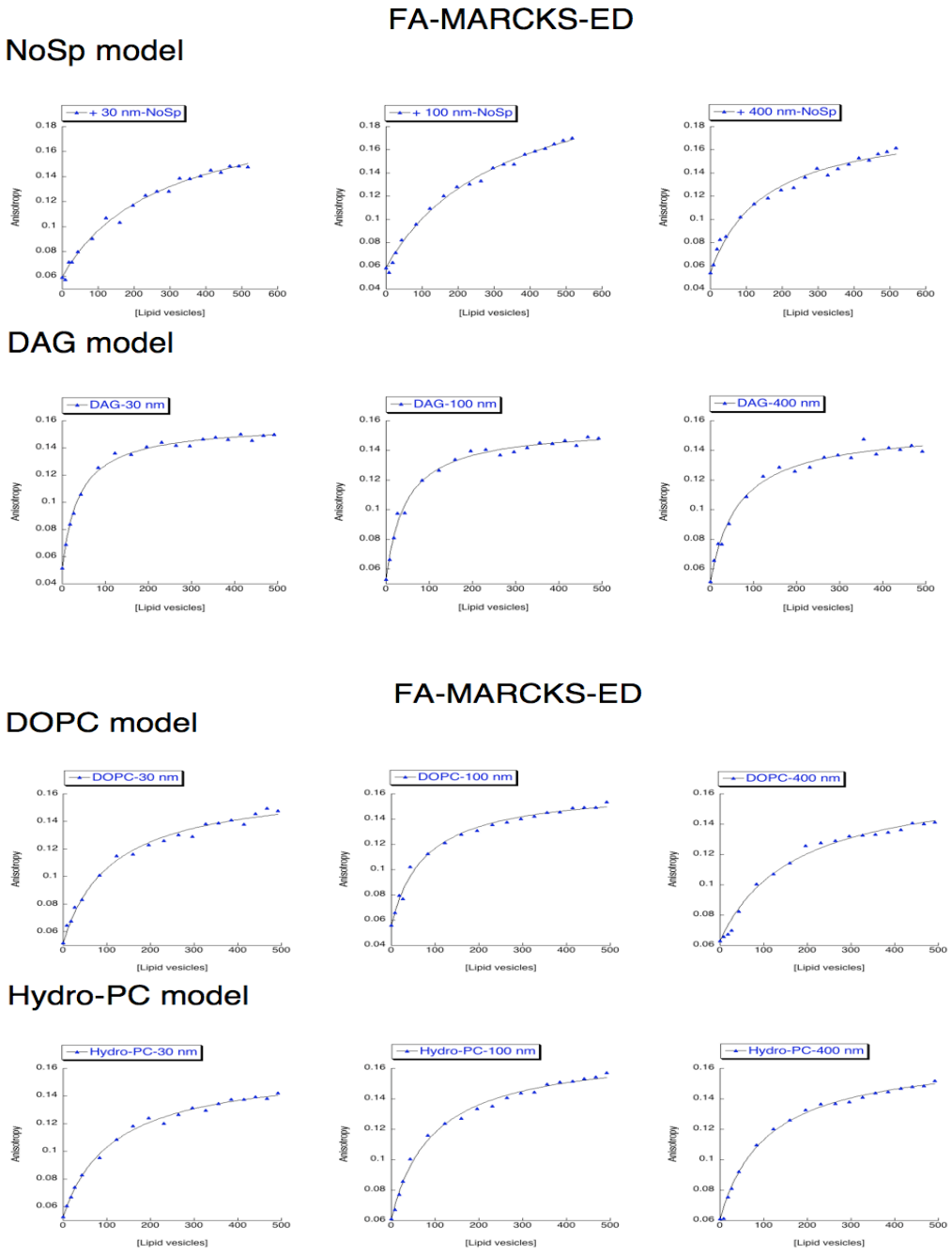

Figure 4.11 Anisotropy plots of FA-MARCKS-ED with different lipid models described in Table 4.1 and Figure 4.7. Lipid models include: NoSp, DAG, DOPC and Hydro-PC.

4.5 Discussion.

In this current report, the roles of both the peptide and the lipids were explored. MARCKS-ED adopts an extended, unstructured conformation in solution. Its membrane association is mainly driven by electrostatic interactions. As electrostatic interactions are not configuration-dependent, one may expect that the unnatural D-MARCKS-ED would behave similarly to its natural L-counterpart. Thus it is somewhat surprising that D-MARCKS-ED did not exhibit the curvature selectivity. Experimental and computational studies are underway to investigate these stereo-specific interactions by MARCKS-ED.

The behavior of the peptide points to the important roles that Phe residues play in MARCKS-ED-membrane interaction. EPR is a well-established method to study membrane protein insertion (*18*). Consistent with our speculation that the insertion of Phe residues are critical to the preferential binding of MARCKS-ED to highly curved membranes, we observed a trend that shows a deeper insertion of Phe as the lipid vesicle gets smaller.

In our approach to uncover the influence that membrane composition may have in the curvature sensing behavior of MARCKS-ED, the results suggest that changes in the lipid head group area and lipid packing are major influences in the interaction of the bilayer with MARCKS-ED. PE, with its small head group, can create surface defects and lipid gaps on the surface for larger vesicle sizes. However, to produce surface defects in smaller vesicles, the presence of defect-inducing lipids is not as critical as they are in larger vesicles. This is due to the fact that, for smaller vesicles, the higher surface curvature in itself induces defects to be formed. As can be seen from Figure 4.7a, the removal of PE did not result to a significant

change in MARCKS-ED binding to the 30- and 100-nm vesicles. The presence of PE can affect the detection of PS on the surface of bilayers (*58*) and this could be the reason for the stronger binding of MARCKS-ED to the 400-nm vesicle once PE has been removed. Our hypothesis was that DAG could rescue this curvature sensing behavior in the absence of PE due to its structural shape. Similar to PE, the smaller head group of DAG would allow for more access for hydrophobic insertion and perhaps interfering with electrostatic interactions for larger vesicles. However, the replacement of PE with DAG shows no significant rescue of curvature sensing. This suggests that although DAG and PE have smaller head groups relative to their lipid tails, these two lipid components do not behave similarly. This could be due to the lack of the negatively charged phosphate group in the DAG head group that makes its behavior markedly different from that of PE. Interestingly, the FA-MARCKS-ED peptide showed strong binding affinities for the DAG lipid model relative to the other lipid models. Taken together, no curvature sensing behavior was observed for either peptide with this mutant model, indicating the essential role that PE plays in the curvature sensing by MARCKS-ED.

Furthermore, the membrane rigidity, which is related to the generation and maintenance of surface defects that arise from lipid packing, appear to influence curvature sensing by MARCKS-ED. Curvature sensing behavior was eliminated upon replacement of cholesterol by phosphatidylcholine, PC. Likewise, the binding of MARCKS-ED to the 30- and 100-nm vesicles did not show an appreciable response to the removal of cholesterol but resulted in tighter binding to the 400-nm. These results suggest that any change that cholesterol may bring about to membrane fluidity has more effect on the largest vesicle than to the two smaller ones. In larger

vesicles, cholesterol may add more fluidity to both stabilize any surface defects that are formed and decrease lipid constraints to allow for better bilayer insertion. On the other hand, the high degree of curvature present in the smaller vesicles can bring about such a degree of lipid packing that the effect of cholesterol becomes unnoticeable. That is, even with the removal of cholesterol, the fluidity of the smaller bilayers is not impacted greatly because of the lipid packing that occurs inherently due to curvature. This may also suggest why the wild type model shows weaker binding for larger vesicles. In contrast to their deletion models, cholesterol and PE could be influencing membrane fluidity and lipid surface defects, which may interfere with electrostatic interactions of larger vesicles. Given previous studies showing PE's influence on PS membrane exposure (*58*), this may explain how MARCKS-ED selectively targets highly curved vesicles with stronger binding affinity in their absence.

The binding affinities revealed by the replacement of cholesterol by Hydro-PC PC (fluidity-decreasing lipids) and DOPC (fluidity-enhancing lipids) in Figure 4.7a also points to the role of lipid packing in membrane bilayers on the curvature sensing behavior of MARCKS-ED. These studies demonstrate how the addition of the fluidity-altering lipids can restore the curvature sensing compromised in cholesterol-deficient lipid vesicles. However, the head group sizes characteristic of each lipid could have an effect on the induction of surface defects. As with the results above shown with PE and DAG, this could affect the charge distribution of PS and thus, affect MARCKS-ED binding.

Results observed for the FA-MARCKS-ED mutant peptide displayed weaker binding compared to the wild type MARCKS-ED peptide, and importantly without membrane curvature

distinction. These results further confirmed the importance of Phe insertion in both MARCKS-ED membrane binding and curvature sensing.

Extracellular vesicle shedding spontaneously occurs with both normal and cancer cells. Their primary function is to promote cell-to-cell communication and to deliver vital proteins as cargo, which is dependent on the cell from which it was derived from (*12*). Most interestingly, these nano-sized highly curved membranes are over-expressed in those with cancer and have been recently linked to cancer progression (*12*). The correlation to cancer progression stems from its functions of promoting angiogenesis for cancer cells, modulating the tumor microenvironment, evading the immune system with over-exposed phosphatidylserine and resisting chemotherapeutic drugs (*9*). For cancer cells, these functions support tumor survival and proliferation as these spontaneous vesicles spread to other parts of the body, transporting through bodily fluids such as blood, urine and tissue fluid (*9*). Understanding how to target highly curved membranes gives us an edge to transfer this knowledge to create potential peptide probes to target biologically relevant highly curved extracellular vesicles, which could be used to monitor cancer progression. These peptides could serve as noninvasive sensors to monitor the spread and transport of these extracellular vesicles in those with cancer to improve prognostic decisions.

Using experimental biophysical techniques, we have probed the mechanism underlying the curvature sensing ability of MARCKS-ED. This was done by examining alterations in curvature sensing behavior brought about by changes in both the peptide and the bilayers. The results of this study contribute to the formulation of fundamental rules that govern the interaction between proteins and curved membranes. This will positively impact the identification and

rational design of novel proteins and peptides that, in their ability to target highly curved vesicles, can be used for various future biological applications.

Chapter 5

Conclusions and Future Works on Fully Characterizing MARCKS-ED's Curvature Sensing Behavior as well as Identifying Other Curvature Sensing Peptides

5.1 Conclusions.

This work has focused on dissecting specific factors that contribute to curvature sensing behavior between proteins and membranes, using a rationally chosen peptide. Peptides were chosen for this project due to their feasibility for molecular dynamic studies and their noninvasive properties. Also, our focus was to uncover the specific molecular contributions involved with curvature sensing behavior: another reason to use peptides to isolate these intermolecular interactions with the membrane. To create an efficient assay to optimally isolate peptide-membrane interactions, we designed a defined protocol to produce and extrude different lipid vesicle sizes. Our bio-analytical techniques including dynamic light scattering and nanoparticle tracking analysis measured results to validate our extrusion method, displaying a linear correlation between the vesicle polycarbonate membrane pores used for extrusion versus the quantitative diameter measured by the software and observed on the distribution curve. This method is a significant branch of this work since the accuracy and precision of synthetic lipid vesicle production of distinct sizes does indeed influence subsequent binding assays.

The MARCKS-ED peptide was chosen primarily based on its known behavior to bind to the membrane to acidic lipids driven by electrostatic interactions. Interestingly, Morton et al.

identified a novel behavior of the MARCKS-ED peptide binding preferentially to highly curved membrane surfaces. This novel observation was displayed in an assortment of assays, including *in vitro* and *ex vivo* fluorescence assays. Synthetic lipid vesicles of different diameter sizes ranging from 30-400 nm were titrated to a MARCKS-ED solution to measure the binding affinity, generating stronger binding to the smallest vesicle size. Furthermore, we generated MARCKS-ED mutant peptides: (1) mutating all Arg, Lys basic residues to Ala residues, (2) mutating all Phe residues to Ala residues and (3) representing a scrambled MARCKS-ED sequence. Fluorescence measured compromised binding for all mutant peptides, demolishing curvature sensing behavior for mutants 1 and 2. Interestingly, mutant 3 did show curvature sensing behavior despite the loss in binding.

Following the fluorescence assays which confirmed the cosedimentation pull-down assay that MARCKS-ED prefers highly curved vesicles, our focus turned to using biologically relevant highly curved vesicles. These vesicles are commonly recognized as exosomes and microvesicles, collectively known as extracellular vesicles that shed from cells and circulate throughout the body for cellular communication. Using fluorescence and the nanoparticle tracking analysis, the MARCKS-ED peptide displayed a greater degree of binding for vesicles <100 nm in diameter. Based on the unique lipid environment of these biological vesicles of increased PS, we performed *in vivo* experiments using an established *C. elegans* model to further confirm MARCKS-ED's interaction with these shed extracellular vesicles. These results and observations led us to further try and understand these interactions by asking how much is MARCKS-ED's curvature sensing behavior based on the specificity of the peptide as well as on the lipid

composition.

Our second question was to understand this newly identified MARCKS-ED behavior. Based on previous studies reporting Phe hydrophobic insertion for MARCKS-ED, we proposed that this mechanism may be influencing curvature sensing behavior. Furthermore, several lipid studies indicate their unique control over membrane shape, mobility and morphology. Experiments were carried out to answer these two speculative ideas on curvature sensing behavior. Electron paramagnetic resonance (EPR) was performed to identify any importance of Phe insertion for curvature sensing behavior. These studies suggested that the MARCKS-ED peptide is more likely to be found closer to the membrane bilayer of smaller vesicles relative to larger ones, measuring a greater depth insertion value for smaller vesicles relative to larger ones. Fluorescence assays were carried out using different lipid models with lipid component deletions to determine whether MARCKS-ED required a specific lipid environment for curvature sensing behavior. Phosphatidylethanolamine (PE) and cholesterol deletion lipid models abolished curvature sensing behavior. Our results suggested that lipid composition is important in MARCKS-ED's curvature sensing behavior, proposing that PE and cholesterol may be key factors, further indicating two significant factors: (1) the lipid head group area and (2) membrane fluidity.

5.2 Future Works

5.2.1 Further understanding the roles of PE and cholesterol in MARCKS-ED's curvature sensing behavior. Our focus on understanding how lipid components influence MARCKS-ED's

curvature sensing behavior led us to observe unexpected results regarding two particular lipid components. Tighter binding affinities for all sizes of 30-, 100- and 400 nm vesicles was observed using fluorescence anisotropy with lipid models where PE and cholesterol were replaced with phosphatidylcholine (PC). In contrast, the wild type lipid model measured weaker binding affinity for the 400 nm relative to both the 30- and 100 nm vesicle solutions. We considered this difference in binding affinity to be significant based on at least a 1.9 fold difference in K_D. This particular definition to distinguish membrane curvature is based on Hui et al.'s studies on identifying Synaptotagmin-1 as a curvature sensing protein (*3*). Our fluorescence results suggested that both PE and cholesterol could be influencing membrane packing, surface defects and phosphatidylserine (PS) exposure for larger vesicles, influencing how MARCKS-ED interacts with larger vesicles. Our results simply suggest their contributions to MARCKS-ED's curvature sensing behavior but further studies would be helpful to fully understand the specific roles PE and cholesterol have in curvature sensing behavior. One suggestion would be to study lipid dynamics and their behavior in membrane bilayers of different curvatures to further understand how these lipid components influence membrane packing and fluidity in contrast to other lipids. Furthermore, future work should include studies using a double mutant lipid model, e.g. NoPE and NoCh.

5.2.2. Using EPR for mutant lipid models. As described in Chapter 4, EPR is a technique to measure the depth parameter value in membrane bilayers. The studies explained in this chapter describe different sizes using the wild type model containing all lipid components. Based

on the current lipid fluorescence results revealing the importance of PE and cholesterol, further EPR studies using lipid models replacing PE and cholesterol with PC may reveal differences in how MARCKS-ED inserts into the membrane without these lipid components. If indeed both PE and cholesterol affect membrane packing, MARCKS-ED may insert differently with these mutant lipid models relative to what was observed for the wild type model as described in Chapter 4. Since fluorescence assays have already revealed differences in MARCKS-ED's curvature sensing behavior, conducting EPR studies with these mutant models may also reveal further understanding of membrane curvature sensing and the contribution of certain lipids in observing this behavior.

5.2.3 Improving and optimizing curvature sensing behavior of the MARCKS-ED peptide. More studies will be carried out to fully characterize and improve how MARCKS-ED targets positive curvature. Based on known curvature sensing proteins, oligomerization has been recognized as a potential factor for certain proteins to sense positive membrane curvature based on how multiple protein units can provide enhanced scaffolding of the membrane surface (*1*). One idea to answer whether MARCKS-ED's curvature sensing behavior could be enhanced is to oligomerize the MARCKS-ED peptide. This approach would include synthesizing multiple MARCKS-ED peptide units and designing a clever scaffold to connect these units.

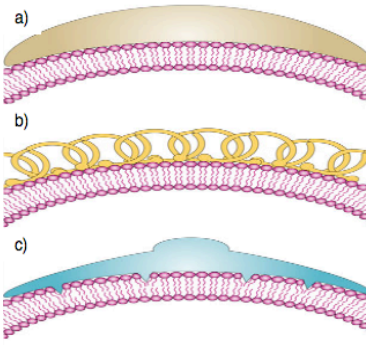

Scheme 5.1 Schematic depiction of how proteins and peptide structural and molecular moieties may influence membrane curvature sensing. Describes a) a scaffolding mechanism, b) oligomerization and c) hydrophobic molecular insertion. This scheme is courtesy of Zimmerberg et al (*27*).

5.2.4 Characterizing the D-MARCKS-ED peptide.

Another way to maybe unveil further understanding of the MARCKS-ED peptide is to use its mirror image, D-MARCKS-ED, with D-form amino acids to undergo similar studies as the natural L-form of MARCKS-ED. Few studies have been performed using D-MARCKS-ED as displayed from Chapter 4, which showed contrasting behavior than the wild type peptide. These studies however were preliminary and further work could elucidate more structural understanding of how MARCKS-ED selectively targets highly curved vesicles.

5.2.5 Identifying other potential curvature sensing peptides. Based on the intrinsic properties recently identified in the MARCKS-ED peptide that allow curvature sensing behavior, other short peptides can be selected for comparison containing the following: (a) basic residues

to stabilize itself on the membrane surface via electrostatic interactions, (b) evenly distributed hydrophobic residues for membrane bilayer insertion and (c) perhaps oligomerization may help. One such peptide that may be of future interest is derived from a secretory carrier membrane protein (SCAMP), where the peptide is known as SCAMP-E. SCAMP proteins are four membrane-spanning helical proteins involved with membrane fusion during exocytosis (*16*). This highly conserved sequence, CWYRPIYKAFR, is derived from the short cytoplasmic segment linking the second and third transmembrane helices. Similar to MARCKS-ED, this peptide also binds to membrane surfaces with exposed regions of phophatidylinositol 4,5-bisphosphate, $PI(4,5)P_2$. The PIP_2 sequestration mechanism of these PIP_2 lipid molecules on the cytoplasmic inner leaflet mirrors MARCKS-ED's natural, biological behavior. Based on our findings from MARCKS-ED, SCAMP-E's highly basic and hydrophobic, aromatic residues could provide the necessary contributions to observe curvature sensing behavior. Furthermore, SCAMP-E's sequence consist of a central Pro residue, proposing a more interesting configuration that could create a scaffold upon membrane binding. Slightly shorter than MARCKS-ED, the 11-residue peptide has also been shown to insert into the membrane bilayer, proposing that its aromatic residues are found in the lipid hydrocarbon region, but has not currently been recognized as a curvature sensing peptide.

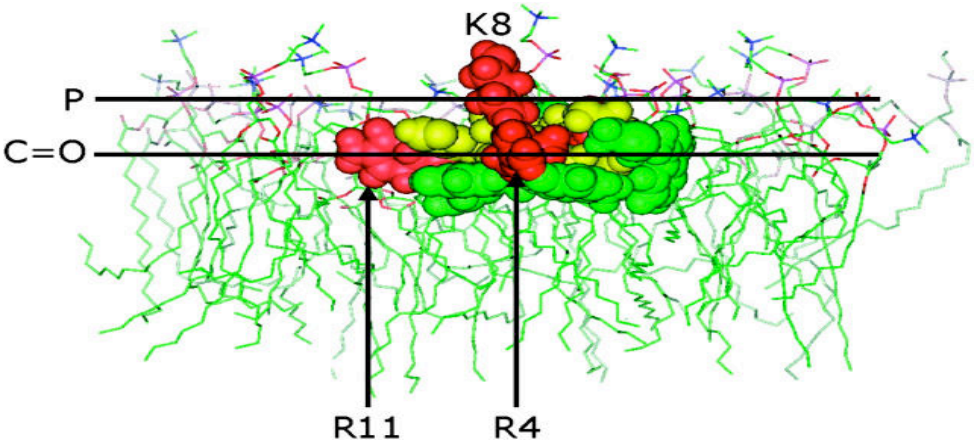

Scheme 5.2 Schematic depiction showing SCAMP-E bound to the membrane bilayer. This model, which included PC lipids, was generated from data courtesy of Cafiso et al and Armen et al (*16, 59*).

BIBLIOGRAPHY:

1. McMahon, H. T., and Gallop, J. L. (2005) Membrane curvature and mechanisms of dynamic cell membrane remodelling, *Nature 438*, 590-596.

2. Nikos S Hatzakis, V. K. B., Jannik Larsen, Kenneth L Madsen, Pierre-Yves Bolinger, Andreas H Kunding, John Castillo, Ulrik Gether, Per Hedegard, Dimitrios Stamou. (2009) How curved membranes recruit amphipathic helices and protein anchoring motifs, *Nature Chemical Biology 5*, 835-841.

3. Hui, E., Johnson, C. P., Yao, J., Dunning, F. M., and Chapman, E. R. (2009) Synaptotagmin-mediated bending of the target membrane is a critical step in Ca(2+)-regulated fusion, *Cell 138*, 709-721.

4. Gerlach, H., Laumann, V., Martens, S., Becker, C. F., Goody, R. S., and Geyer, M. HIV-1 Nef membrane association depends on charge, curvature, composition and sequence, *Nat Chem Biol 6*, 46-53.

5. Drin, G., Casella, J. F., Gautier, R., Boehmer, T., Schwartz, T. U., and Antonny, B. (2007) A general amphipathic alpha-helical motif for sensing membrane curvature, *Nat Struct Mol Biol 14*, 138-146.

6. Low, C., Weininger, U., Lee, H., Schweimer, K., Neundorf, I., Beck-Sickinger, A. G., Pastor, R. W., and Balbach, J. (2008) Structure and dynamics of helix-0 of the N-BAR domain in lipid micelles and bilayers, *Biophys J 95*, 4315-4323.

7. Bhatia, V. K., Madsen, K. L., Bolinger, P. Y., Kunding, A., Hedegard, P., Gether, U., and Stamou, D. (2009) Amphipathic motifs in BAR domains are essential for membrane curvature sensing, *EMBO J 28*, 3303-3314.

8. Ginestra, A., La Placa, M. D., Saladino, F., Cassara, D., Nagase, H., and Vittorelli, M. L. (1998) The amount and proteolytic content of vesicles shed by human cancer cell lines correlates with their in vitro invasiveness, *Anticancer Res 18*, 3433-3437.

9. Muralidharan-Chari, V., Clancy, J. W., Sedgwick, A., and D'Souza-Schorey, C. Microvesicles: mediators of extracellular communication during cancer progression, *J Cell Sci 123*, 1603-1611.

10. Poste, G., and Nicolson, G. L. (1980) Arrest and metastasis of blood-borne tumor cells are modified by fusion of plasma membrane vesicles from highly metastatic cells, *Proc Natl Acad Sci U S A 77*, 399-403.

11. Cocucci, E., Racchetti, G., and Meldolesi, J. (2009) Shedding microvesicles: artefacts no more, *Trends Cell Biol 19*, 43-51.

12. Camussi, G., Deregibus, M. C., Bruno, S., Cantaluppi, V., and Biancone, L. (2010) Exosomes/microvesicles as a mechanism of cell-to-cell communication, *Kidney Int 78*, 838-848.

13. Dragovic, R. A., Gardiner, C., Brooks, A. S., Tannetta, D. S., Ferguson, D. J., Hole, P., Carr, B., Redman, C. W., Harris, A. L., Dobson, P. J., Harrison, P., and Sargent, I. L. (2011) Sizing and phenotyping of cellular vesicles using Nanoparticle Tracking Analysis, *Nanomedicine 7*, 780-788.

14. Kim, J., Blackshear, P. J., Johnson, J. D., and McLaughlin, S. (1994) Phosphorylation reverses the membrane association of peptides that correspond to the basic domains of MARCKS and neuromodulin, *Biophys J 67*, 227-237.

15. Rusu, L., Gambhir, A., McLaughlin, S., and Radler, J. (2004) Fluorescence correlation spectroscopy studies of Peptide and protein binding to phospholipid vesicles, *Biophys J 87*, 1044-1053.

16. Ellena, J. F., Moulthrop, J., Wu, J., Rauch, M., Jaysinghne, S., Castle, J. D., and Cafiso, D. S. (2004) Membrane position of a basic aromatic peptide that sequesters phosphatidylinositol 4,5 bisphosphate determined by site-directed spin labeling and high-resolution NMR, *Biophys J 87*, 3221-3233.

17. Yamauchi, E., Nakatsu, T., Matsubara, M., Kato, H., and Taniguchi, H. (2003) Crystal structure of a MARCKS peptide containing the calmodulin-binding domain in complex with Ca2+-calmodulin, *Nat Struct Biol 10*, 226-231.

18. Qin, Z., and Cafiso, D. S. (1996) Membrane structure of protein kinase C and calmodulin binding domain of myristoylated alanine rich C kinase substrate determined by site-directed spin labeling, *Biochemistry 35*, 2917-2925.

19. Kim, J., Shishido, T., Jiang, X., Aderem, A., and McLaughlin, S. (1994) Phosphorylation, high ionic strength, and calmodulin reverse the binding of MARCKS to phospholipid vesicles, *J Biol Chem 269*, 28214-28219.

20. Ellena, J. F., Burnitz, M. C., and Cafiso, D. S. (2003) Location of the myristoylated alanine-rich C-kinase substrate (MARCKS) effector domain in negatively charged phospholipid bicelles, *Biophys J 85*, 2442-2448.

21. Zhang, W., Crocker, E., McLaughlin, S., and Smith, S. O. (2003) Binding of peptides with basic and aromatic residues to bilayer membranes: phenylalanine in the myristoylated alanine-rich C kinase substrate effector domain penetrates into the hydrophobic core of the bilayer, *J Biol Chem 278*, 21459-21466.

22. Morton, L. A., Yang, H., Saludes, J. P., Fiorini, Z., Beninson, L., Chapman, E. R., Fleshner, M., Xue, D., and Yin, H. MARCKS-ED peptide as a curvature and lipid sensor, *ACS Chem Biol 8*, 218-225.

23. Mui, B., Chow, L., and Hope, M. J. (2003) Extrusion technique to generate liposomes of defined size, *Methods Enzymol 367*, 3-14.

24. Loughrey, H. C., Choi, L. S., Cullis, P. R., and Bally, M. B. (1990) Optimized procedures for the coupling of proteins to liposomes, *J Immunol Methods 132*, 25-35.

25. Gruner, S. M., Cullis, P. R., Hope, M. J., and Tilcock, C. P. (1985) Lipid polymorphism: the molecular basis of nonbilayer phases, *Annu Rev Biophys Biophys Chem 14*, 211-238.

26. Guven, A., Ortiz, M., Constanti, M., and O'Sullivan, C. K. (2009) Rapid and efficient method for the size separation of homogeneous fluorescein-encapsulating liposomes, *J Liposome Res 19*, 148-154.

27. Zimmerberg, J., and Kozlov, M. M. (2006) How proteins produce cellular membrane curvature, *Nat Rev Mol Cell Biol 7*, 9-19.

28. Connor, J., Bucana, C., Fidler, I. J., and Schroit, A. J. (1989) Differentiation-dependent expression of phosphatidylserine in mammalian plasma membranes: quantitative assessment of outer-leaflet lipid by prothrombinase complex formation, *Proc Natl Acad Sci U S A 86*, 3184-3188.

29. Smith, S. A., and Morrissey, J. H. (2004) Rapid and efficient incorporation of tissue factor into liposomes, *J Thromb Haemost 2*, 1155-1162.

30. Chonn, A., and Cullis, P. R. (1995) Recent advances in liposomal drug-delivery systems, *Curr Opin Biotechnol 6*, 698-708.

31. Mayer, L. D., Hope, M. J., and Cullis, P. R. (1986) Vesicles of variable sizes produced by a rapid extrusion procedure, *Biochim Biophys Acta 858*, 161-168.

32. K. Matsuoka, R. S. (2001) The use of liposomes to study COPII- and COPI-coated vesicle formation and membrane protein sorting, *Methods 20*, 417-428.

33. Hunter, D. G., and Frisken, B. J. (1998) Effect of extrusion pressure and lipid properties on the size and polydispersity of lipid vesicles, *Biophys J 74*, 2996-3002.

34. Morton, L. A., Saludes, J. P., and Yin, H. Constant Pressure-controlled Extrusion Method for the Preparation of Nano-sized Lipid Vesicles, *J Vis Exp 64*, e4151.

35. Mesmin, B., Drin, G., Levi, S., Rawet, M., Cassel, D., Bigay, J., and Antonny, B. (2007) Two lipid-packing sensor motifs contribute to the sensitivity of ArfGAP1 to membrane curvature, *Biochemistry 46*, 1779-1790.

36. Ouimet, C. C., Wang, J. K., Walaas, S. I., Albert, K. A., and Greengard, P. (1990) Localization of the MARCKS (87 kDa) protein, a major specific substrate for protein kinase C, in rat brain, *J Neurosci 10*, 1683-1698.

37. Wang, J., Gambhir, A., Hangyas-Mihalyne, G., Murray, D., Golebiewska, U., and McLaughlin, S. (2002) Lateral sequestration of phosphatidylinositol 4,5-bisphosphate by the basic effector domain of myristoylated alanine-rich C kinase substrate is due to nonspecific electrostatic interactions, *J Biol Chem 277*, 34401-34412.

38. Madsen, K. L., Bhatia, V. K., Gether, U., and Stamou, D. (2010) BAR domains, amphipathic helices and membrane-anchored proteins use the same mechanism to sense membrane curvature, *FEBS Lett 584*, 1848-1855.

39. Merrifield, R. B. (1963) Merrifield Solid-Phase Peptide Synthesis, *J. Am. Chem. Soc. 85*, 2149.

40. Kaiser, E., Colescott, R. L., Bossinger, C. D., and Cook, P. I. (1970) Color test for detection of free terminal amino groups in the solid-phase synthesis of peptides, *Anal Biochem 34*, 595-598.

41. Rothman, J. E., and Lenard, J. (1977) Membrane asymmetry, *Science 195*, 743-753.

42. Wang, X., Wang, J., Gengyo-Ando, K., Gu, L., Sun, C. L., Yang, C., Shi, Y., Kobayashi, T., Mitani, S., Xie, X. S., and Xue, D. (2007) C. elegans mitochondrial factor WAH-1 promotes phosphatidylserine externalization in apoptotic cells through phospholipid scramblase SCRM-1, *Nat Cell Biol 9*, 541-549.

43. Arbuzova, A., Wang, L., Wang, J., Hangyas-Mihalyne, G., Murray, D., Honig, B., and McLaughlin, S. (2000) Membrane binding of peptides containing both basic and aromatic residues. Experimental studies with peptides corresponding to the scaffolding region of caveolin and the effector region of MARCKS, *Biochemistry 39*, 10330-10339.

44. Matsubara, M., Yamauchi, E., Hayashi, N., and Taniguchi, H. (1998) MARCKS, a major protein kinase C substrate, assumes non-helical conformations both in solution and in complex with Ca2+-calmodulin, *FEBS Lett 421*, 203-207.

45. Peter, B. J., Kent, H. M., Mills, I. G., Vallis, Y., Butler, P. J., Evans, P. R., and McMahon, H. T. (2004) BAR domains as sensors of membrane curvature: the amphiphysin BAR structure, *Science 303*, 495-499.

46. Graves, L. E., Ariztia, E. V., Navari, J. R., Matzel, H. J., Stack, M. S., and Fishman, D. A. (2004) Proinvasive properties of ovarian cancer ascites-derived membrane vesicles, *Cancer Res 64*, 7045-7049.

47. Logozzi, M., De Milito, A., Lugini, L., Borghi, M., Calabro, L., Spada, M., Perdicchio, M., Marino, M. L., Federici, C., Iessi, E., Brambilla, D., Venturi, G., Lozupone, F., Santinami, M., Huber, V., Maio, M., Rivoltini, L., and Fais, S. (2009) High levels of exosomes expressing CD63 and caveolin-1 in plasma of melanoma patients, *PLoS One 4*, e5219.

48. Meers, P., and Mealy, T. (1993) Calcium-dependent annexin V binding to phospholipids: stoichiometry, specificity, and the role of negative charge, *Biochemistry 32*, 11711-11721.

49. Darland-Ransom, M., Wang, X., Sun, C. L., Mapes, J., Gengyo-Ando, K., Mitani, S., and Xue, D. (2008) Role of C. elegans TAT-1 protein in maintaining plasma membrane phosphatidylserine asymmetry, *Science 320*, 528-531.

50. Arkhipov, A., Yin, Y., and Schulten, K. (2009) Membrane-bending mechanism of amphiphysin N-BAR domains, *Biophys J 97*, 2727-2735.

51. McMahon, H. T., and Gallop, J. L. (2005) Membrane curvature and mechanisms of dynamic cell membrane remodelling, *Nature 438*, 590-596.

52. Shemesh, T., Luini, A., Malhotra, V., Burger, K. N., and Kozlov, M. M. (2003) Prefission constriction of Golgi tubular carriers driven by local lipid metabolism: a theoretical model, *Biophys J 85*, 3813-3827.

53. van Meer, G., Voelker, D. R., and Feigenson, G. W. (2008) Membrane lipids: where they are and how they behave, *Nat Rev Mol Cell Biol 9*, 112-124.

54. Laulagnier, K., Motta, C., Hamdi, S., Roy, S., Fauvelle, F., Pageaux, J. F., Kobayashi, T., Salles, J. P., Perret, B., Bonnerot, C., and Record, M. (2004) Mast cell- and dendritic cell-

derived exosomes display a specific lipid composition and an unusual membrane organization, *Biochem J 380*, 161-171.

55. Rubenstein, J. L., Smith, B. A., and McConnell, H. M. (1979) Lateral diffusion in binary mixtures of cholesterol and phosphatidylcholines, *Proc Natl Acad Sci U S A 76*, 15-18.

56. Hofsass, C., Lindahl, E., and Edholm, O. (2003) Molecular dynamics simulations of phospholipid bilayers with cholesterol, *Biophys J 84*, 2192-2206.

57. Rawicz, W., Olbrich, K. C., McIntosh, T., Needham, D., and Evans, E. (2000) Effect of chain length and unsaturation on elasticity of lipid bilayers, *Biophys J 79*, 328-339.

58. Shi, J., Pipe, S. W., Rasmussen, J. T., Heegaard, C. W., and Gilbert, G. E. (2008) Lactadherin blocks thrombosis and hemostasis in vivo: correlation with platelet phosphatidylserine exposure, *Journal of Thrombosis and Haemostasis 6*, 1167-1174.

59. Armen, R. S., Uitto, O. D., and Feller, S. E. (1998) Phospholipid component volumes: determination and application to bilayer structure calculations, *Biophys J 75*, 734-744.

60. Saludes, J. P., Morton, L. A., Ghosh, N., Beninson, L. A., Chapman, E. R., Fleshner, M., and Yin, H. Detection of highly curved membrane surfaces using a cyclic peptide derived from synaptotagmin-I, *ACS Chem Biol 7*, 1629-1635.

61. Saludes, J. P., Morton, L. A., Coulup, S. K., Fiorini, Z., Cook, B. M., Beninson, L., Chapman, E. R., Fleshner, M., and Yin, H. Multivalency amplifies the selection and affinity of bradykinin-derived peptides for lipid nanovesicles, *Mol Biosyst 9*, 2005-2009.

62. Bigay, J., Casella, J. F., Drin, G., Mesmin, B., and Antonny, B. (2005) ArfGAP1 responds to membrane curvature through the folding of a lipid packing sensor motif, *EMBO J 24*, 2244-2253.

Appendix I

My contributions towards two other curvature sensing peptides are described and both identified by Dr. Jonel P. Saludes.

These studies were published in the following papers:

1-Saludes, J.P.; Morton, L. A.; Ghosh, N.; Beninson, L.; Chapman, E.; Fleshner, M. and Yin, H. (2012) Detection of Highly Curved Membrane Surfaces Using a Cyclic Peptide Derived from Synaptotagmin-1, ACS Chem. Biol. 7, 1629-1635.

2-Saludes, J. P.; Morton, L. A.; Coulup, S.; Fiorini, Z.; Cook, B. M.; Beninson, L.; Chapman, E. R.; Fleshner, M. and Yin, H. (2013) Multivalency Amplifies the Selection and Affinity of Bradykinin-Derived Peptide for Lipid Nanovesicles, Mol BioSyst.; 9, 2005-2009.

A.1 Summary of the C2B peptide.

A truncated sequence from the C2B domain of the membrane fusion protein Synaptotagmin-1 (Syt-1) was rationally chosen as a potential curvature sensing peptide. Syt-1 is currently recognized as a curvature sensing protein as it is an important component of the Soluble N-ethylmaleimide-sensitive factor Attachment protein Receptor (SNARE) complex, which modulates calcium-dependent membrane fusion, neurotransmitter release and hormone secretion (*3*). This behavior is reported to be the result of an insertion mechanism that includes stabilizing interactions between Ca^{2+} ions and flexible loops located at the ends of both C2A and C2B domains of the Syt-1 protein. Surprisingly, biophysical studies revealed no curvature sensing behavior with this linear, unstructured 10-residue peptide (DYDKIGKNDA), known as the C2B

peptide, derived from loop 3 of the C2B domain. Further work however did show that rigidity properties were necessary for this behavior after a cyclic C2B peptide was generated, measuring higher binding affinities for highly curved vesicles relative to the linear C2B peptide.

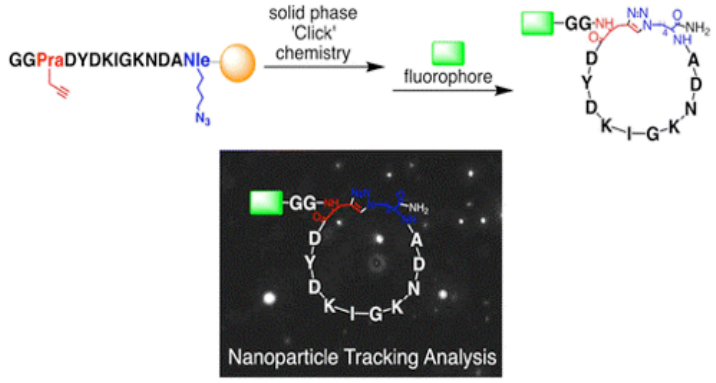

Scheme A.1 Schematic of cyclizing the linear C2B peptide using "Click Chemistry". Curvature sensing behavior was observed for the cyclized C2B peptide in contrast to the linear form. This scheme is courtesy of Saludes et al (*60*).

A.2 Contribution 1: C2B.

My contribution to this work included a role in characterizing the vesicle diameter using the known technique dynamic light scattering (DLS) for identifying and measuring the hydrodynamic radii of particles based on fluctuations of light scatter influenced by their Brownian motion. As mentioned earlier, it is important to produce homogeneous solutions of distinct vesicle sizes. Determining the accurate vesicle diameter following our extrusion method gives validity to our conclusions on identifying peptides that exhibit curvature sensing behavior. DLS was performed for each synthetic lipid vesicle solution after extrusion through polycarbonate membrane pores. These values were recorded and then plotted in calibration

graphs shown in the supplementary information of Saludes et al (*60*).

A.3 Summary of the Bradykinin peptide.

The Bradykinin peptide was rationally chosen for curvature sensing studies based on its unique peptide sequence including an important proline, which could presumably provide a scaffold for selectively targeting highly curved membrane surfaces. The Bradykinin peptide is a cationic ligand for B1 and B2 G-protein coupled receptors and its sequence is described in Scheme A.2. Based on solid-state NMR spectroscopy and molecular dynamics, reports show the Bradykinin peptide undergoing a conformational change upon membrane interaction. Specifically, a B-turn conformation is induced which consequently orients the arginine residues, R1 and R9, in a 'claw-like' shape, perhaps critical for membrane binding. Furthermore, previous reports suggest that Bradykinin's insertion mechanism into the membrane bilayer is electrostatically-driven. Based on the above characteristics of the Bradykinin peptide, biophysical studies were carried out to identify any curvature sensing behavior. The results (*61*) showed that the monomeric Bradykinin peptide revealed selective curvature behavior with weaker binding affinity for the larger vesicles relative to the smaller ones. Even more interestingly, a trimeric Bradykinin peptide was synthesized and prepared to study whether multivalency of a curvature sensing peptide could improve curvature sensing behavior. Fluorescence polarization revealed a five-fold difference in binding strength for the trimeric Bradykinin peptide relative to the monomeric form.

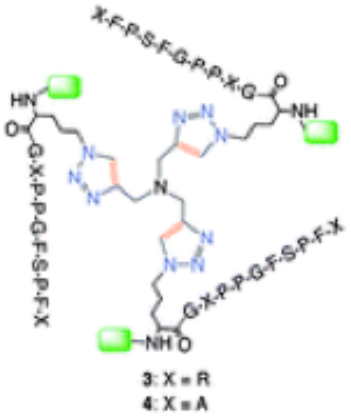

Scheme A.2 Schematic of generating the trimeric form made up of three monomeric units of Bradykinin, XFPSFGPPX (where X = R for wild type and A for mutant). The extra G on the N-terminus was added as a linker prior to the NBD label conjugation. The trimer peptide produced stronger binding affinities among all vesicle sizes relative to the monomer form as well as indicated curvature sensing behavior. This scheme is courtesy of Saludes et al (*61*).

A.4 Contribution 2: Bradykinin.

My contribution to this work included performing fluorescence anisotropy polarization using the mutant Bradykinin peptide where the Arg residues were mutated to Ala residues. Furthermore, the Bradykinin peptide was synthesized and chemically arranged into a trimeric molecule using an established technique referred to as “Click Chemistry”. The results showed stronger binding for highly curved vesicles for the trimer Bradykinin peptide relative to the monomer Bradykinin peptide. Fluorescence anisotropy measured weak binding curves for the mutant trimer, where the arginine residues were mutated to alanine residues. In fact, the apparent dissociation constants of the mutant Bradykinin trimer were similarly weak for all lipid vesicle solutions regardless of

vesicle curvature. Fluorescence anisotropy was integral in displaying any curvature sensing properties for the Bradykinin peptide as it exposed the significance of the arginine residues in membrane interaction and subsequently membrane curvature sensing.

A.5 Conclusions.

Two curvature sensing peptides, formally recognized as the C2B and Bradykinin peptides, were identified in our focus to better understand membrane-peptide interactions. These peptides were rationally chosen based on different properties stemming from previously known curvature sensing proteins. It is important to note that our interest in peptide-based studies in contrast to protein-based studies is based on the following preferred peptide features: (1) stability, (2) modifiability and (3) computational-feasibility. The C2B peptide conveyed the importance of structural stability allowing it to insert into lipid bilayers of highly curved vesicles. The Bradykinin peptide expressed how shape may also play a role in selecting for highly curved vesicles as its critical arginine residues were shown to be necessary for membrane interaction. Upon lipid vesicle interaction, the arginine residues are proposed to orient themselves into a 'claw-like' shape on the membrane. Although both of these newly-identified curvature sensing peptides required contrasting characteristics, e.g. loop rigidity and conformational shape relative to the MARCKS-ED peptide, these studies give insight into curvature sensing behavior. Both the C2B and Bradykinin peptides use their unique features to insert into the membrane bilayer of highly curved vesicles; a common property shared with the MARCKS-ED peptide.

Appendix II

Identifying lipid concentration effects

B.1 Determination of lipid concentrations.

Lipid concentration is critical to curvature sensing studies. Different lipid concentration can alter binding effects upon interaction by the MARCKS-ED peptide. Indeed, the lipid concentration obtained in these studies were inscribed and recorded on each vial purchased and received by Avanti Polar Lipids. To mathematically confirm and measure lipid concentration, the number of total lipid molecules can be determined based on the equation described in Equation B.1. The number of the total lipid molecules can be converted into moles by dividing by Avogadro's number, e.g. 6.02×10^{23} molecules in 1 mole. Specifically, lipid concentration is defined as the lipid amount, moles in this case, divided by a certain volume. The number of lipid molecules can be determined based on the lamellarity of the lipid vesicle, which can be determined by 31P-NMR spectroscopy. In fact, it has been proposed that lipid vesicles of 100 nm are considered unilamellar. Knowing the lipid composition is also critical for knowing the area of the head group, which is required to determine the number of lipid molecules in the vesicle solution.

$$N_{total} = [4\pi(d/2)^2 + 4\pi(d/2 - h)^2] / a$$

Equation B.1 Solving for the total amount of lipid molecules in a lipid vesicle solution. This equation describes how the total number of lipid molecules in a lipid vesicle solution can be determined based on knowing (a) the lamellarity of the vesicle as well as (b) the lipid component used. In this equation, the surface area for each monolayer of the lipid vesicle is measured, where

both are added together. The total lipid area is then divided by the surface area of the lipid head group. The variables are defined as the following: d, diameter of the lipid vesicle; h, lipid bilayer known as 5 nm; a, lipid head group area. This information and equation is courtesy of Encapsula NanoSciences obtained from www.encapsula.com.

B.2 Lipid concentration measurements in binding assays.

During sample preparation, the lipid concentration was determined based on measurements that had been previously performed for the ArfGAP1 protein with small vesicles to show a 1:1000 ratio of peptide:lipid vesicle concentration (*62*). To acquire a sufficient fluorescence response for our fluorescence enhancement assays, our peptide concentration did not fall below 500 nM. To sustain a 1:1000 ratio, we chose a lipid vesicle concentration of 500 μM. We indeed observed preferential binding of the MARCKS-ED peptide to smaller vesicles relative to larger ones, most optimally with 10% phosphatidylserine. To quantify this binding, we prepared a MARCKS-ED solution approximately 10-fold lower, 1 μM, than the predicted dissociation constant. Our predictions were based on previous reports of micromolar affinity between MARCKS-ED and lipid vesicles with monovalent acidic phospholipids (*14*). The lipid concentration solution was prepared at 2 mM. This prepared solution was highly concentrated to ensure binding saturation according to the Michaelis-Menten equation and its assumptions. These assumptions suggest that at higher concentrated lipid vesicle solutions relative to the MARCKS-ED peptide concentration, all MARCKS-ED peptide molecules are assumed to be bound to the lipid vesicles at binding saturation: where no free peptide should exist in solution. Furthermore, in our cosedimentation

assay, the lipid concentration closely resembled the lipid concentration used for the fluorescence enhancement assay; however, higher amounts of the MARCKS-ED peptide were required in order to optimally observe the peptide on the SDS gel.

B.3 Different MARCKS-ED concentration effects on lipid vesicles in binding assays.

With higher than normal MARCKS-ED peptide concentrations used for our cosedimentation assay, altering effects can be proposed based on the data observed. A cosedimentation pull-down assay was performed; previously preformed by other groups to identify curvature sensing behavior (*3*). In this data, we observed more MARCKS-ED peptide was pulled down after high speeds of ultra-centrifugation (75K rpm) after incubation with small vesicles (d=100 nm) relative to incubation with large vesicles (d=400 nm). This data appears to show very little of the 400 nm vesicles being pulled down by the MARCKS-ED peptide, suggesting more than a 2-fold binding difference between the two different vesicle sizes. An approximate 2-fold binding difference was observed for the curvature sensing protein Synaptotagmin-1 between small vesicles (d=105 nm; K_D = 151 μM) and large vesicles (d=252 nm; K_D = 283 μM). In fact, in both fluorescence enhancement and anisotropy assays, binding was observed with the larger 400 nm vesicles but with lower fluorescence intensity and at weaker binding affinity than the smaller 30 nm vesicles. Observations of binding could be due to the sensitivity of the fluorescence assays, which are based on the change surrounding the fluorophore environment. Although similar lipid concentration was used for the cosedimentation assay (600 μM) relative to the fluorescence enhancement assay (500 μM), the dissociation constants from the anisotropy assay revealed that

the lipid concentration required for 50% of the MARCKS-ED peptide to bind ranged between 24 ± 3 μM, 42 ± 13 μM and 86 ± 20 μM (*22*). These results show more than a 2-fold binding affinity difference between the 30 and 400 nm vesicles. In fact, this ~3.5 fold difference may reflect on why we see such a drastic difference between the two vesicle sizes of 100 and 400 nm in our cosedimentation assay.

Indeed the lack of binding for the larger 400 nm vesicles observed in the cosedimentation assay could be a result of higher than normal MARCKS-ED peptide concentrations. It has been observed that at high MARCKS-ED concentrations, vesicle tubulation can occur with the MARCKS-ED peptide based on negative staining transmission electron microscopy (TEM) images (Figure B.1). This is rationally proposed based on the cationic residues of the sequence, which can behave to fuse and aggregate vesicles highly exposed with anionic lipids. These cosedimentation results could indeed be reflecting curvature sensing; however, we cannot rule out that the possibility of tubulation occurring with these lipid vesicles. As observed in Figure B.1, tubulation was observed in vesicles of all sizes at high concentrations of MARCKS-ED (10 μM). More assays were performed following the cosedimentation assay considering the high concentration of MARCKS-ED required which could affect the behavior of the MARCKS-ED when interacting with lipid vesicles. This assay was only performed to first observe if MARCKS-ED could potentially be showing preferential binding, but other assays were conducted to confirm this behavior.

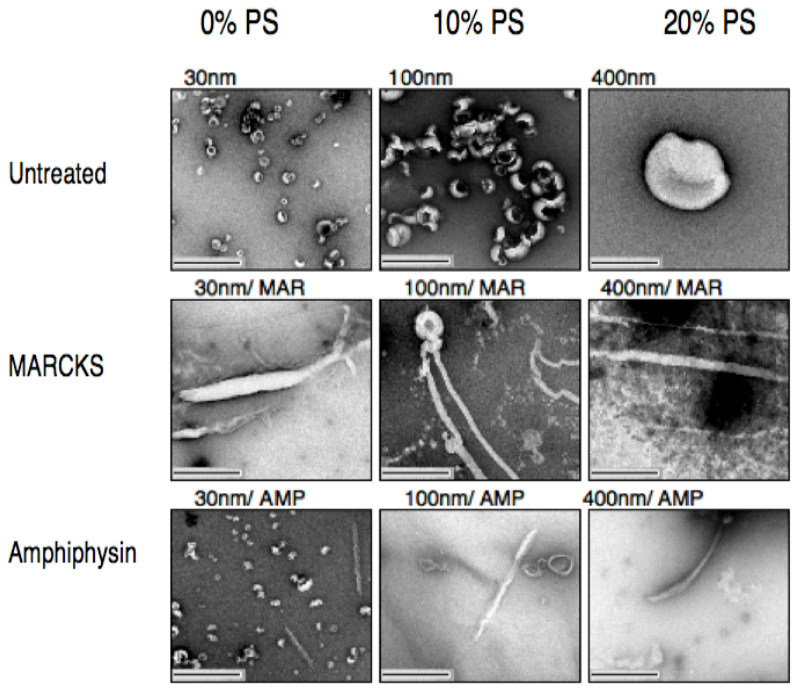

Figure B.1 Negative stain transmission electron microscopy (TEM) of vesicle tubulation of MARCKS-ED peptide. Incubation of MARCKS-ED peptide with lipid vesicles creates lipid vesiculation with vesicles at varying concentrations of phosphatidylserine. These images were performed in parallel with Amphiphysin, a known curvature sensing protein containing the N-BAR domain, the amphipathic helix-0 on the N-terminus of the BAR domain, responsible for inducing curvature. [MARCKS-ED] = 10 μM; [Amphiphysin] = 10 μM; [Lipid vesicle] = 500 μM. Scale bar = 0.40 μm. Magnification = ×34000.

B.4 Potential lipid concentration effects from lipid extrusion.

Furthermore, it is possible that lipid concentration can be altered during the lipid vesicle preparation. Indeed, we use an optimal extrusion technique where we alter the nitrogen flow to produce homogenous solutions of different vesicle sizes (*34*). It is possible however to modify the lipid concentration after one extrusion, leaving some remaining lipid molecules in the extrusion chamber. This could have effects on determining the conclusions of our binding results. Specifically, in Figure 4.10, the mutant FA-MARCKS-ED peptide showed preferential binding to the 340 nm vesicles over the 100 and 30 nm vesicles for the wild type model. Although this behavior is in contrast to what we observed for the wild type MARCKS-ED peptide, this could conclude that the FA-MARCKS-ED peptide may have bound tighter to the larger 400 nm vesicles if the concentration for these 400 nm vesicles was higher relative to the 30 nm vesicles. Less nitrogen is required to pass lipid vesicle solution through the extruder to produce larger vesicles based on the large pore size. In contrast, more nitrogen is required to pass liquid solution through the extrusion chamber for vesicles of much smaller diameter pore sizes; thus, more pressure is required to pass lipids through the extrusion chamber possibly excluding some lipid molecules unable to pass through the chamber. Knowing this, it is possible that more lipid molecules could have been present in this particular larger vesicle solution relative to the smaller vesicle solution, thus, affecting binding saturation with the FA-MARCKS-ED peptide for each vesicle solution.

It is important to mention however that multiple passes are carried out for each vesicle size, 3-5 times, during the extrusion process in order to produce homogenous solutions that do

not vary in lipid concentration. In fact, the same molar percentage for each lipid composition should exist in each lipid vesicle size solution. To determine and confirm this, the nanoparticle tracking analysis can be performed to measure the number of particles in each solution. If the mole amount of lipids is consistent, more particles should be observed for the smaller vesicles relative to the larger ones based on the amount of lipids required to produce different sized lipid vesicles.